**The following notice applies to any unclassified (including originally classified and now declassified) technical reports released to "qualified U.S. contractors" under the provisions of DoD Directive 5230.25, Withholding of Unclassified Technical Data From Public Disclosure.**

**NOTICE TO ACCOMPANY THE DISSEMINATION OF EXPORT-CONTROLLED TECHNICAL DATA**

**1. Export of information contained herein, which includes, in some circumstances, release to foreign nationals within the United States, without first obtaining approval or license from the Department of State for items controlled by the International Traffic in Arms Regulations (ITAR), or the Department of Commerce for items controlled by the Export Administration Regulations (EAR), may constitute a violation of law.**

**2. Under 22 U.S.C. 2778 the penalty for unlawful export of items or information controlled under the ITAR is up to ten years imprisonment, or a fine of $1,000,000, or both. Under 50 U.S.C., Appendix 2410, the penalty for unlawful export of items or information controlled under the EAR is a fine of up to $1,000,000, or five times the value of the exports, whichever is greater; or for an individual, imprisonment of up to 10 years, or a fine of up to $250,000, or both.**

**3. In accordance with your certification that establishes you as a "qualified U.S. Contractor", unauthorized dissemination of this information is prohibited and may result in disqualification as a qualified U.S. contractor, and may be considered in determining your eligibility for future contracts with the Department of Defense.**

**4. The U.S. Government assumes no liability for direct patent infringement, or contributory patent infringement or misuse of technical data.**

**5. The U.S. Government does not warrant the adequacy, accuracy, currency, or completeness of the technical data.**

**6. The U.S. Government assumes no liability for loss, damage, or injury resulting from manufacture or use for any purpose of any product, article, system, or material involving reliance upon any or all technical data furnished in response to the request for technical data.**

**7. If the technical data furnished by the Government will be used for commercial manufacturing or other profit potential, a license for such use may be necessary. Any payments made in support of the request for data do not include or involve any license rights.**

**8. A copy of this notice shall be provided with any partial or complete reproduction of these data that are provided to qualified U.S. contractors.**

**DESTRUCTION NOTICE**

**For classified documents, follow the procedure in DoD 5220.22-M, National Industrial Security Program, Operating Manual, Chapter 5, Section 7, or DoD 5200.1-R, Information Security Program Regulation, Chapter 6, Section 7. For unclassified, limited documents, destroy by any method that will prevent disclosure of contents or reconstruction of the document.**

AD NUMBER

**AD475190**

LIMITATION CHANGES

TO:

**Approved for public release; distribution is unlimited.**

FROM:

**Distribution authorized to U.S. Gov't. agencies and their contractors; Critical Technology; SEP 1965. Other requests shall be referred to Air Force Flight Dynamic Laboratory, Attn: FDFR, AFB, OH 45433. This document contains export-controlled technical data.**

AUTHORITY

**AFFDL ltr, 24 Jan 1973**

# SECURITY MARKING

**The classified or limited status of this report applies to each page, unless otherwise marked.**
**Separate page printouts MUST be marked accordingly.**

THIS DOCUMENT CONTAINS INFORMATION AFFECTING THE NATIONAL DEFENSE OF THE UNITED STATES WITHIN THE MEANING OF THE ESPIONAGE LAWS, TITLE 18, U.S.C., SECTIONS 793 AND 794. THE TRANSMISSION OR THE REVELATION OF ITS CONTENTS IN ANY MANNER TO AN UNAUTHORIZED PERSON IS PROHIBITED BY LAW.

NOTICE: When government or other drawings, specifications or other data are used for any purpose other than in connection with a definitely related government procurement operation, the U. S. Government thereby incurs no responsibility, nor any obligation whatsoever; and the fact that the Government may have formulated, furnished, or in any way supplied the said drawings, specifications, or other data is not to be regarded by implication or otherwise as in any manner licensing the holder or any other person or corporation, or conveying any rights or permission to manufacture, use or sell any patented invention that may in any way be related thereto.

AFFDL-TR-65-108



# DRAG AND STABILITY OF GUIDE SURFACE, RIBBON, AND RINGSLOT PARACHUTES AT HIGH SUBSONIC SPEEDS

*E. L. HAAK*
*R. J. HUBERT*

*UNIVERSITY OF MINNESOTA*

TECHNICAL REPORT . FFDL-TR-65-108

SEPTEMBER 1965



AIR FORCE FLIGHT DYNAMICS LABORATORY
RESEARCH AND TECHNOLOGY DIVISION
AIR FORCE SYSTEMS COMMAND
WRIGHT-PATTERSON AIR FORCE BASE, OHIO

## NOTICES

When Government drawings, specifications, or other data are used for any purpose other than in connection with a definitely related Government procurement operation, the United States Government thereby incurs no responsibility nor any obligation whatsoever; and the fact that the Government may have formulated, furnished, or in any way supplied the said drawings, specifications, or other data, is not to be regarded by implication or otherwise as in any manner licensing the holder or any other person or corporation, or conveying any rights or permission to manufacture, use, or sell any patented invention that may in any way be related thereto.

Qualified users may obtain copies of this report from Defense Documentation Center.

Foreign announcement and dissemination of this report is not authorized.

The distribution of this report is limited because the report contains Technology identifiable with items on the strategic embargo lists excluded from export or re-export under U. S. Export Control Act of 1949 (63 STAT. 7) as amended (50 U.S.C. App. 2020.2031) as implemented by AFR 400-10.

Copies of this report should not be returned to the Research and Technology Division unless return is required by security considerations, contractual obligations, or notice on a specific document.

200 - November 1965 - 18-325-773

# DRAG AND STABILITY OF GUIDE SURFACE, RIBBON, AND RINGSLOT PARACHUTES AT HIGH SUBSONIC SPEEDS

*E. L. HAAK*
*R. J. HUBERT*

*UNIVERSITY OF MINNESOTA*

# FOREWORD

This report was prepared by the Department of Aeronautics and Engineering Mechanics of the University of Minnesota in compliance with U. S. Air Force Contract No. AF 33(657)-11184, "Theoretical Deployable Aerodynamic Decelerator Investigations," Task 606503, "Parachute Aerodynamics and Structures," Project 6065, "Performance and Design of Deployable Aerodynamic Decelerators."

The work accomplished under this contract was sponsored jointly by U. S. Army Natick Laboratory, Department of the Army; Bureau of Aeronautics and Bureau of Ordnance, Department of the Navy; and Air Force Systems Command, Department of the Air Force and was directed by a Tri-Service Steering Committee concerned with Aerodynamic Retardation. The work was administered under the direction of the Recovery and Crew Station Branch, Air Force Flight Dynamics Laboratory, Research and Technology Division. Mr. Rudi J. Berndt and Mr. James H. DeWeese were the project engineers. This effort was funded in part by Air Force Flight Dynamics Laboratory Independent Research Funds.

The authors wish to express their appreciation to Mr. H. D. Davidson, Jr. and to the other personnel at the David Taylor Model Basin, Washington, D.C., who conducted the wind tunnel experiments; to Mr. Joseph Dsida; and to other students of Aerospace Engineering who aided in the accomplishment of this report. The study was conducted under the direction of Prof. H. G. Heinrich.

The manuscript was released by the authors in August 1965 for publication as an RTD technical report.

This technical report has been reviewed and is approved.

GEORGE A. SOLT, JR.
Chief, Recovery and Crew Station Branch
AF Flight Dynamics Laboratory

## ABSTRACT

Four conventional type parachutes, namely, a ribbed and a ribless guide surface parachute and a ribbon and ringslot parachute, were tested at Mach numbers of 0.5 and 0.8 to establish their drag and stability characteristics and to evaluate their general performance in this Mach number range. In all cases the parachute models were stable and their drag coefficients increased slightly with increasing Mach number.

It was found that both the drag and the stability of the guide surface type parachutes change with cloth porosity.

Tests also indicate that for both the ribbed and ribless guide surface parachutes, the tangent force coefficient increases with increasing stagnation pressure at a constant Mach number, and while the stability of the ribless guide surface parachute increases, that of the ribbed type is essentially unchanged.

Tests on ribbon and ringslot parachutes of equal geometric porosity indicate that while the drag increases as the ribbon width increases, the stability of these parachutes does not change significantly with wider ribbons.

The moment coefficients of guide surface parachutes and their derivatives with respect to the angle of attack were in all cases higher than the comparative values of the ribbon or ringslot parachutes.

TABLE OF CONTENTS

## ILLUSTRATIONS

ILLUSTRATIONS (CONT.)

ILLUSTRATIONS (CONT.)

## TABLES

# I. INTRODUCTION

The performance characteristics and the related aerodynamic coefficients of conventional parachutes and their range and mode of variation are fairly well known, especially at low subsonic speeds. Although these parachute types have been used successfully at higher speed for some time, no great deal of analytical and laboratory studies have been performed to evaluate their performance in this flow regime.

The main objective of this study is to establish the aerodynamic coefficients of four conventional parachutes at Mach numbers of 0.5 and 0.8. These endeavors were carried out in wind tunnel studies using scaled models of ribbed and ribless guide surface parachutes and ribbon and ringslot canopies. These studies are similar to an early work performed at a Mach number of 0.1 (Ref 1).

Wherever possible, the measured aerodynamic coefficients have been related to the physical characteristics of the parachute. The cloth porosity was chosen as this characteristic for the guide surface parachutes, and in the case of the ribbon and ringslot parachutes, the aerodynamic coefficients are related to the width of the ribbons from which the canopies are constructed.

Several additional tests were performed to establish parachute performance at various pressure levels and to evaluate drag coefficient changes with Mach number.

The parameters presented in this report can be used for the calculation of the rate of descent and for an approximate determination of the static and dynamic stability depending on the altitude and velocity at which the parachute functions.

# II. EXPERIMENTS

## 1. Coordinate System

In this study the physical coordinates of the parachute are used as the major axis (Fig 1). For this case, the following forces and moments are encountered:

a) The tangent force, T, acting along the centerline of the parachute. This is a drag force at zero angle of attack.

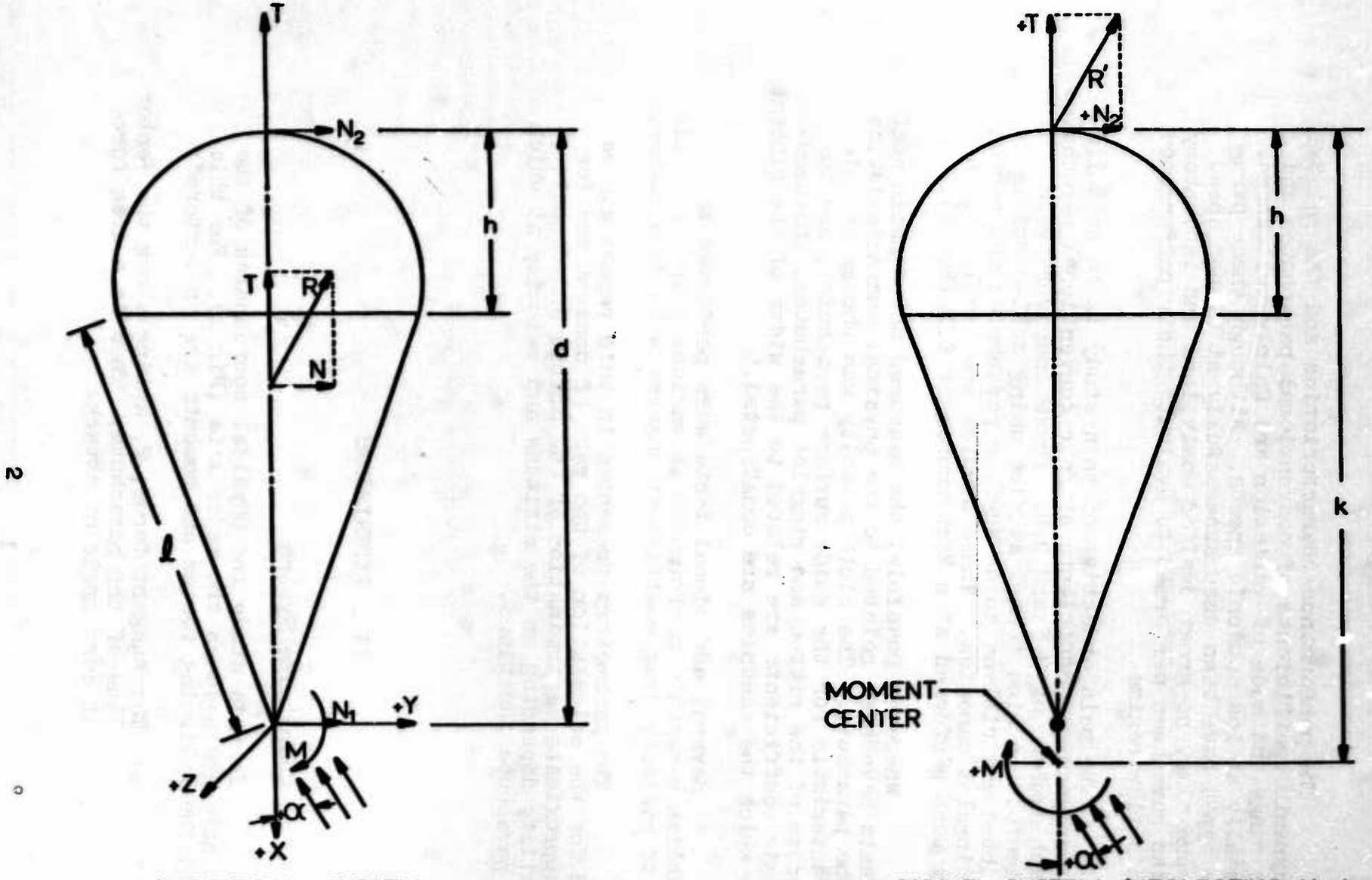


Fig. 1. Parachute Coordinate System and Forces.

b) The normal force, N, acting perpendicular to the parachute centerline.

c) The moment, M, defined as the aerodynamic moment about the nominal confluence point of the parachute suspension lines. The moment is positive when in the same direction as the angle of attack and is stabilizing when the slope $dC_M/d\alpha$ is less than 0 (Ref 2).

## 2. Aerodynamic Coefficients

The force and moment coefficients calculated from the test data employ the conventional relationships:

$$C_T = T/qS$$
$$C_N = N/qS$$
$$C_M = M/qSD \ .$$

If the force $N_1$ in Fig 1A is neglected (Ref 1), then the moment about the nominal parachute confluence point can be calculated as $M = N_2K$ (Fig 1B). The area, S, for the guide surface parachutes is based upon the constructed diameter, $D_C$, and D, the typical length in the moment equation is equal to 1.33 $D_C$. In the case of the ribbon and ringslot parachutes, the total area, $S_o$, and the length $D = D_o = 2\sqrt{S_o/\pi}$ are used.

## 3. Models

### a. Ribbed and Ribless Guide Surface Parachutes

The ribbed and ribless guide surface parachutes have twelve gores and are constructed from the four cloths listed in Table 2 in Appendix A. The ribbed guide surface canopies have a diameter of 12 inches. The ribless guide surface parachutes have a construction diameter, $D_C$, of 12.63 inches. The twelve suspension lines are 200 lb tensile strength nylon (MIL-C-17183, Type III).

### b. Ribbon and Ringslot Parachutes

The ribbon and ringslot models are linearly scaled from 50 to 100 inch prototypes with 20 gores and 20% geometric porosity. The nominal diameter is 16 inches and the suspension lines are nylon cord of 100 lb tensile strength (MIL-C-15020B, Type I). Table 2 in Appendix A summarizes the model specifications.

Since the loads on the canopies at these Mach numbers were expected to be quite high, studies were performed prior to actual wind tunnel testing to establish the

ultimate strength of the canopy and to provide the most desirable confluence point arrangement. From the results of these tests, the maximum loading and, therefore, the maximum wind tunnel pressures were established.

These preliminary tests, the gore patterns, and design details for all parachute models under consideration are presented in Appendix A.

## 4. Experimental Arrangement

The tests were conducted at the Aerodynamic Laboratory, David Taylor Model Basin, Washington, D. C., in the 7' x 10' transonic wind tunnel. This is a continuous flow facility having variable density capability and a digital read-out system for force measurements.

The three component strain gage balance, compatible with existing wind tunnel structure, was designed and built by D.T.M.B. personnel. From previous experience (Ref 1) considerable effort was made to keep the centerline sting as small as possible, and to streamline the upstream structure to avoid any unnecessary flow interference. The tangent force pickup is a small compression member located under the streamlining in the upstream end of the centerline sting (Fig 2A) to which the suspension lines are attached directly. The electrical leads from this element are carried rearward through the centerline sting and into the permanent structure further downstream.

The normal force balance consists of two bending elements placed a known distance apart along the centerline sting in the area of the canopy vent (Fig 2B). When properly oriented and calibrated, this device serves a twofold purpose. First, the sum of the forces in the two elements yields directly the total normal force produced by the parachute. Second, knowing the two individual components, the vent location can be established. Thus, the canopy and suspension line length, d, is directly evaluated.

The tangent force system was designed to measure loads up to 600 lbs, and two normal force elements were constructed for ranges of 0 to 30 lbs and 0 to 120 lbs.

The centerline sting (Fig 2C) is attached to a larger boom extending in the flow direction and attached to a strut further downstream. The entire system was mounted in the tunnel in such a way as to provide the necessary angle of attack range.

## 5. Test Procedure

Stagnation pressures of approximately one half atmosphere were chosen to insure the dynamic pressure would

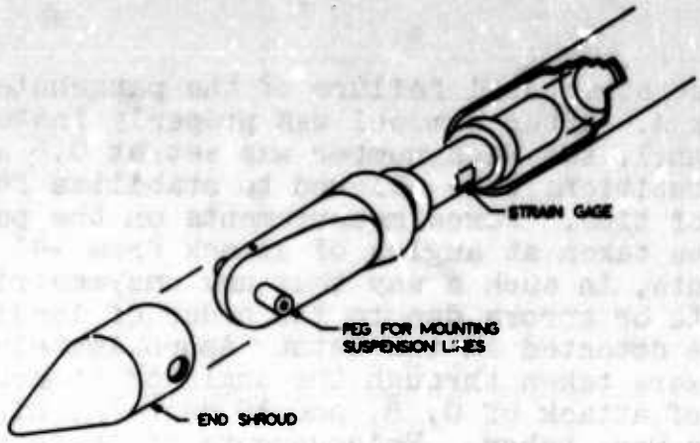


A) DETAIL OF CONFLUENCE POINT

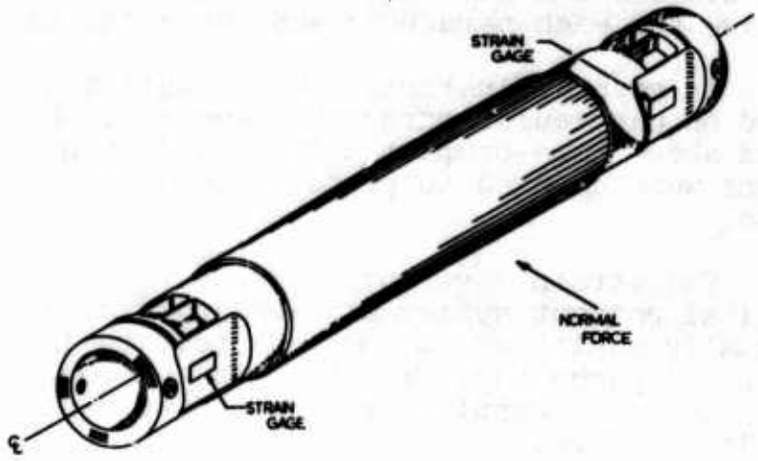


B) DETAIL OF NORMAL FORCE MEASURING DEVICE

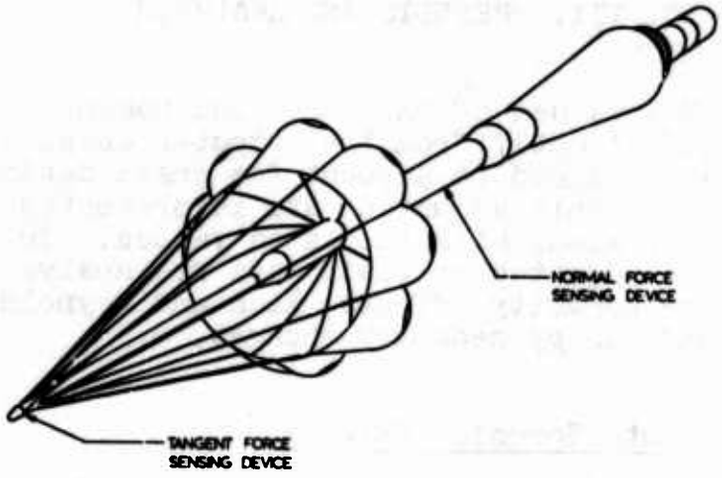


C) PARACHUTE MOUNTED ON THREE COMPONENT STING BALANCE

# Fig 2 Wind Tunnel Balance System

not cause structural failure of the parachute canopies, Appendix A. After a model was properly installed in the wind tunnel, the Mach number was set at 0.5 and the operating conditions were allowed to stabilize for a sufficient length of time. Force measurements on the parachute model were then taken at angles of attack from -4° to +10° in 2° increments, in such a way that any unsymmetries of the parachute or errors due to the order of loading the balance would be detected in the data. Approximately fifteen data points were taken through the angle of attack range. At angles of attack of 0, 6, and 10 degrees, high speed motion pictures were taken. Enlargements of these pictures for two parachutes are shown in Fig 3.

The wind tunnel speed was then increased to Mach number = 0.8 and the same procedure was repeated. The in-tunnel time for each parachute was approximately one hour.

In several instances where additional tests were performed on particular parachute canopies, the basic tests described above were completed first and then wind tunnel conditions were changed to produce the desired mode of operation.

The strain gage outputs were recorded directly on a digital readout system at each angle of attack and were visually monitored during each test to insure proper operation. A punch tape from the digital readout system was utilized by a computer, programmed to reduce the data to coefficient form.

## III. RESULTS AND ANALYSIS

The values of the force and moment coefficients were plotted directly from the computer outputs and then adjusted and aligned to account for small deviations in the raw data. This adjusted data is presented in the graphs in Appendix B along with tabulated values. In the following sections the adjusted or basic data are analyzed in view of effective porosity effects, Mach and Reynolds number effects, and canopy geometry changes.

### 1. Cloth Porosity Effects

The ribless and ribbed guide surface parachutes were constructed of cloth having effective porosity* values

* A comprehensive definition and discussion of effective porosity may be found in Ref 3.

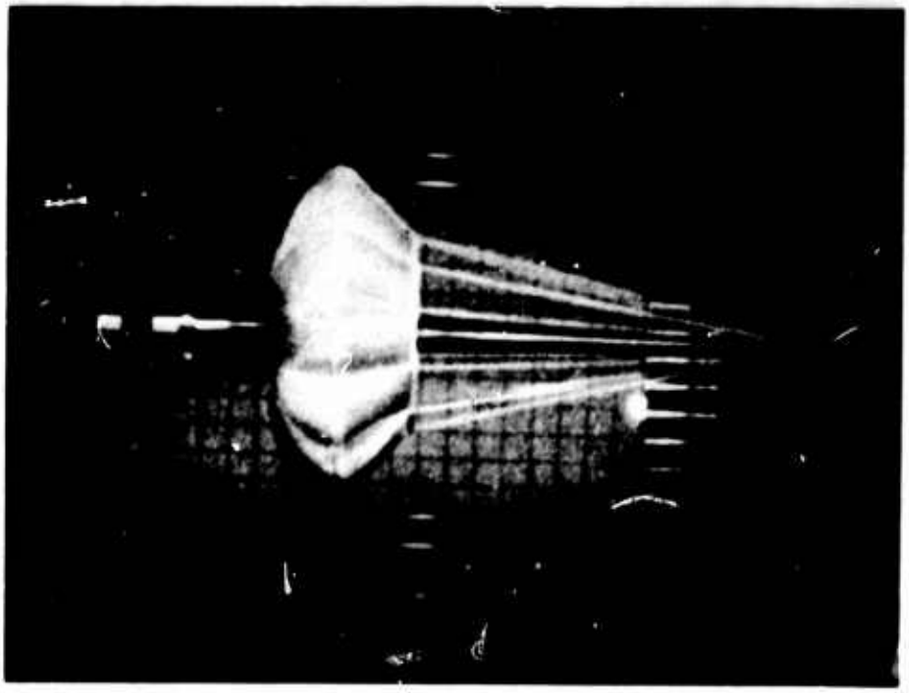

A) RIBBED GUIDE SURFACE, 60 NOMINAL POROSITY
$\alpha = 0$, $M = 0.8$

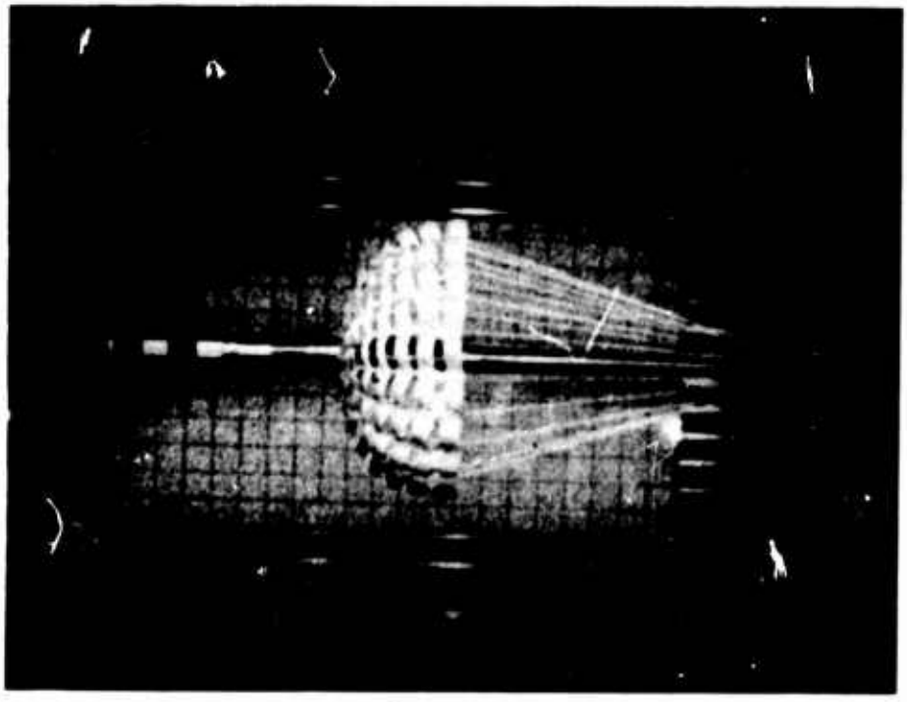

B) RINGSLOT, 50IN PROTOTYPE, $\alpha = 0$, $M = 0.5$

**Fig 3 Parachutes During Wind Tunnel Operation**

ranging from 0.003 to 0.049 as noted in Table 2 in Appendix A. Since all of the parachute canopies tested in this effort were stable at zero angle of attack, a comparison of the aerodynamic coefficients at this condition appears to be sufficient. Figure 4 shows the tangent force coefficient versus effective porosity for the guide surface canopies. For both the test conditions of Mach = 0.5 and Mach = 0.8, the drag or tangent force coefficient increases with increasing cloth porosity. This general trend was also observed in Ref 1.

The stability derivative, $dC_M/d\alpha$, has also been plotted versus porosity as shown in Fig 5. A change in stability is evident as the effective porosity is increased. The stability of the low porosity canopies is not noticeably affected by a Mach number increase but stronger stability is indicated with higher Mach number for the more porous canopies.

## 2. Pressure Effects

In an attempt to gain some insight into the effects of upstream pressure upon parachute canopies, one ribless and one ribbed guide surface parachute were tested over a range of wind tunnel stagnation pressure conditions. The Mach number was held constant at M = 0.5. The 120 nominal porosity ribless guide surface data (Fig 6) shows a measurable increase in the tangent force coefficient and increased stability as pressure increases. The ribbed guide surface canopy (Fig 7) shows some increase in tangent coefficient as pressure increases, but little variation of moment coefficient is noted.

Changes in stagnation pressure imply comparable changes in Reynolds number; however, the effective porosity also varies with pressure level (Fig 8) and it is possible that the canopy shape is also altered. Although the effective porosity is Reynolds number sensitive (Ref 3), the changes in shape can in no way be directly associated with Reynolds number.

In-tunnel measurements from photographs at M = 0.5 and M = 0.8 (Fig 9) show that the ribless guide surface canopies are somewhat susceptible to diameter changes at various test conditions, while the diameter of the ribbed type canopies remains constant. Since the ribbed guide surface parachutes contain a certain amount of supporting structure, this would be expected.

Thus, the data is understood to be primarily dependent on changes in shape which are influenced by stagnation pressure levels. If and in which manner the Reynolds number is involved can not be clearly stated at this time.

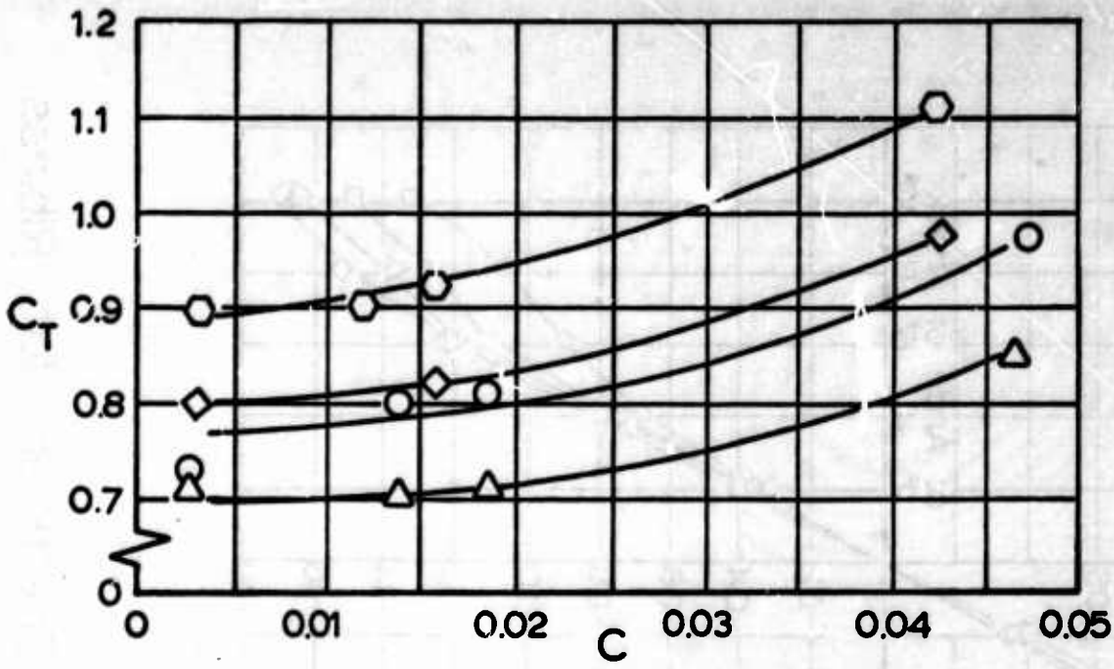


Fig. 4 Tangent Force Coefficient as a Function of Effective Porosity for Guide Surface Parachutes ($\alpha=0$)

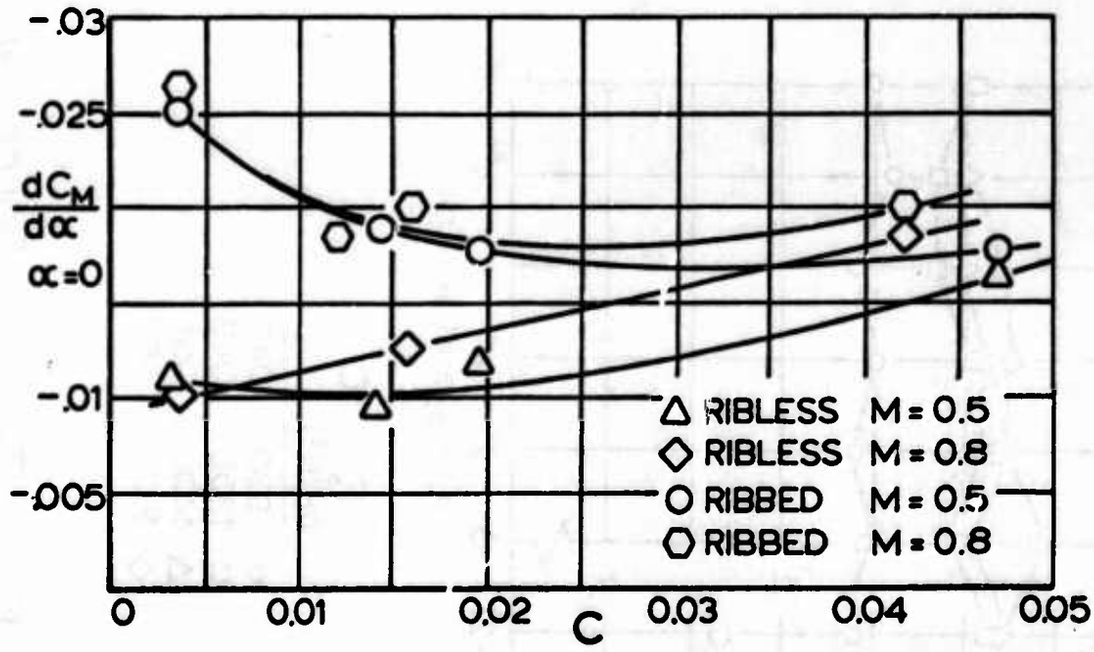


Fig. 5 $dC_M/d\alpha$ as a Function of Effective Porosity for Guide Surface Parachutes ($\alpha=0$)

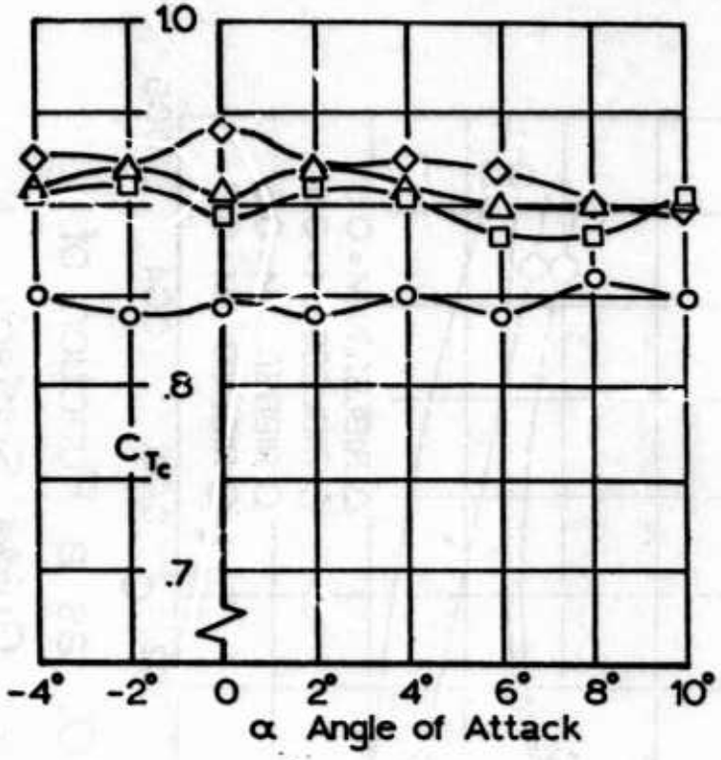


| | $P_o$ (lb/ft²) | C |
|---|---|---|
| ○ | 930 | .047 |
| □ | 1200 | .049 |
| △ | 1400 | .051 |
| ◇ | 1600 | .052 |

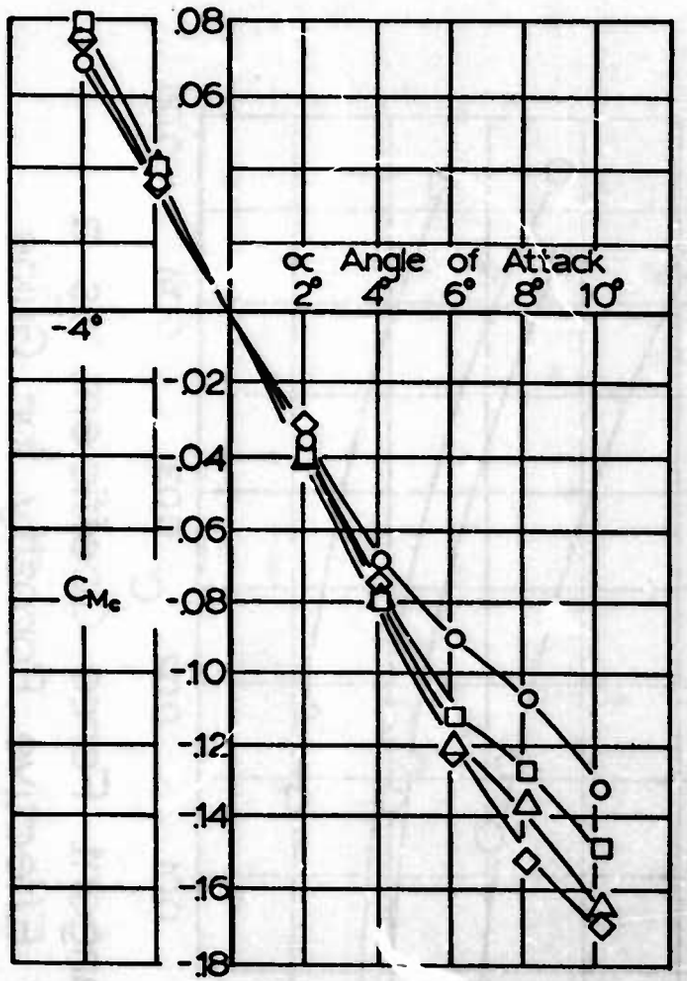


Fig 6 Tangent Force and Moment Coefficient for Ribless Guide Surface Parachute at Various Stagnation Pressures (Nominal Porosity =120 $ft^3/ft^2$ min.)

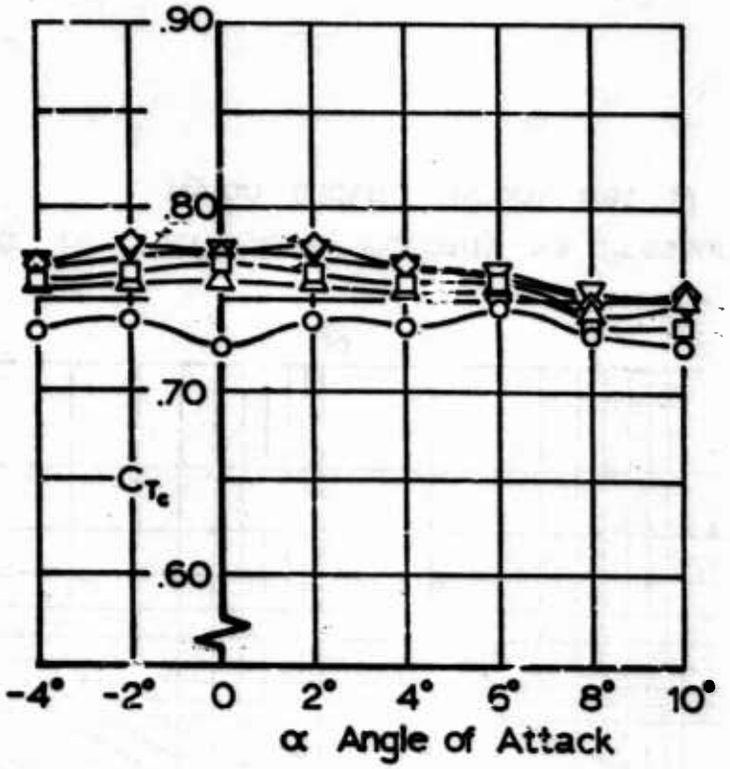


| | $P_o$ (lb/ft²) | C |
|---|---|---|
| ○ | 930 | .018 |
| □ | 1200 | .019 |
| △ | 1400 | .020 |
| ◇ | 1600 | .020 |
| ▽ | 1800 | .021 |

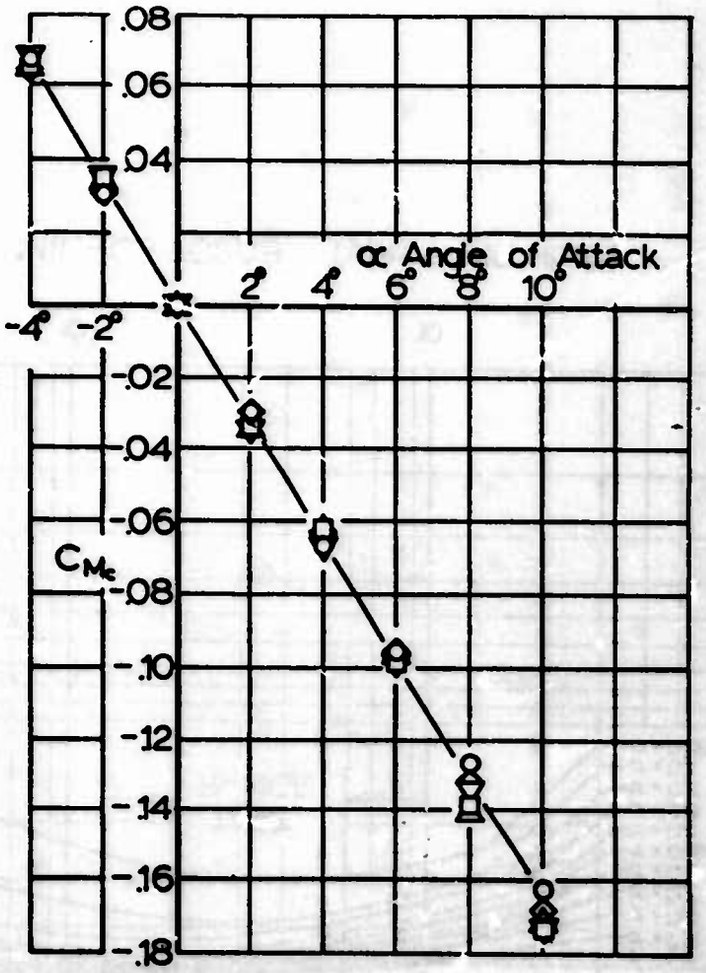


Fig. 7 Tangent Force and Moment Coefficient for Ribbed Guide Surface Parachute at Various Stagnation Pressures ( Nominal Porosity = 60 $ft.^3/ft.^2$ min.)

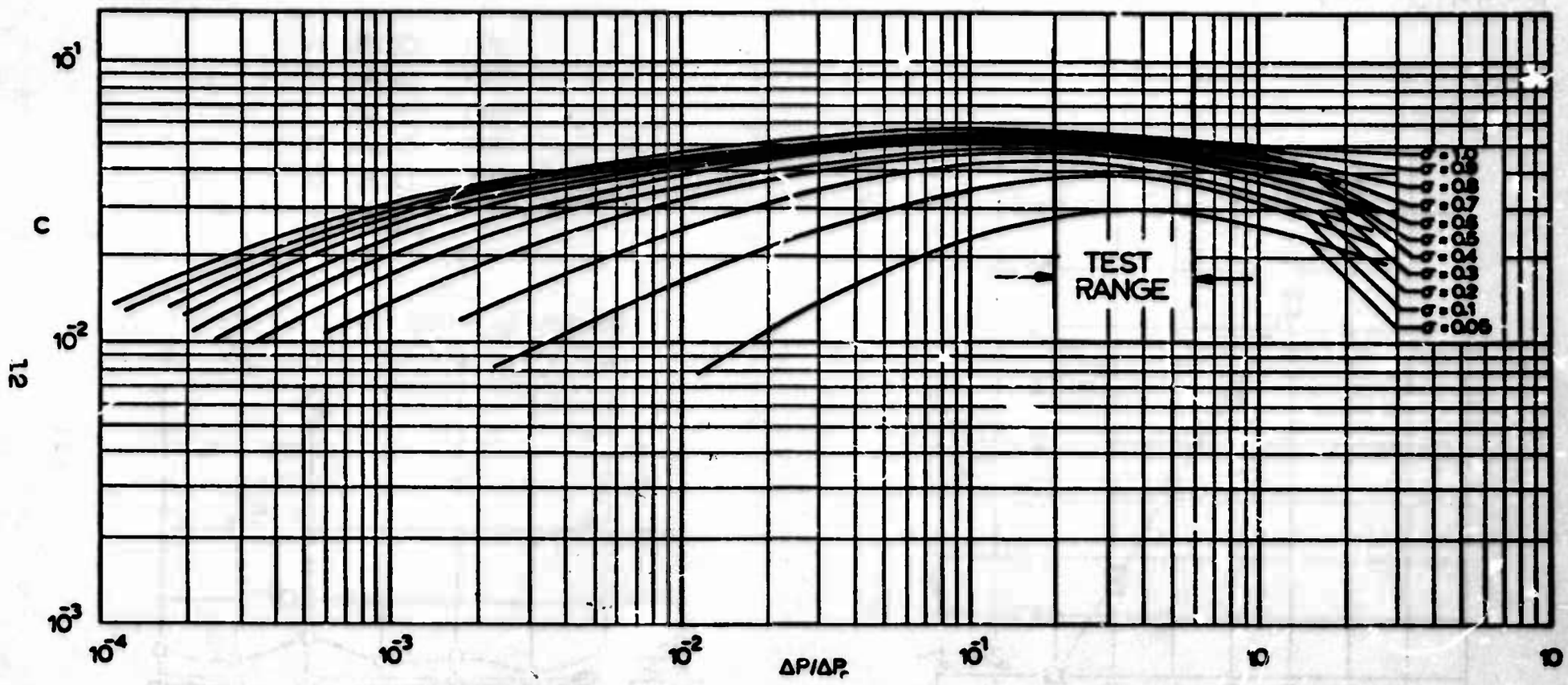


Fig. 8. Effective Porosity vs. Pressure Ratio for MIL-C-7020B, Type I 40 lb/in. Nylon Cloth (From Ref 3)

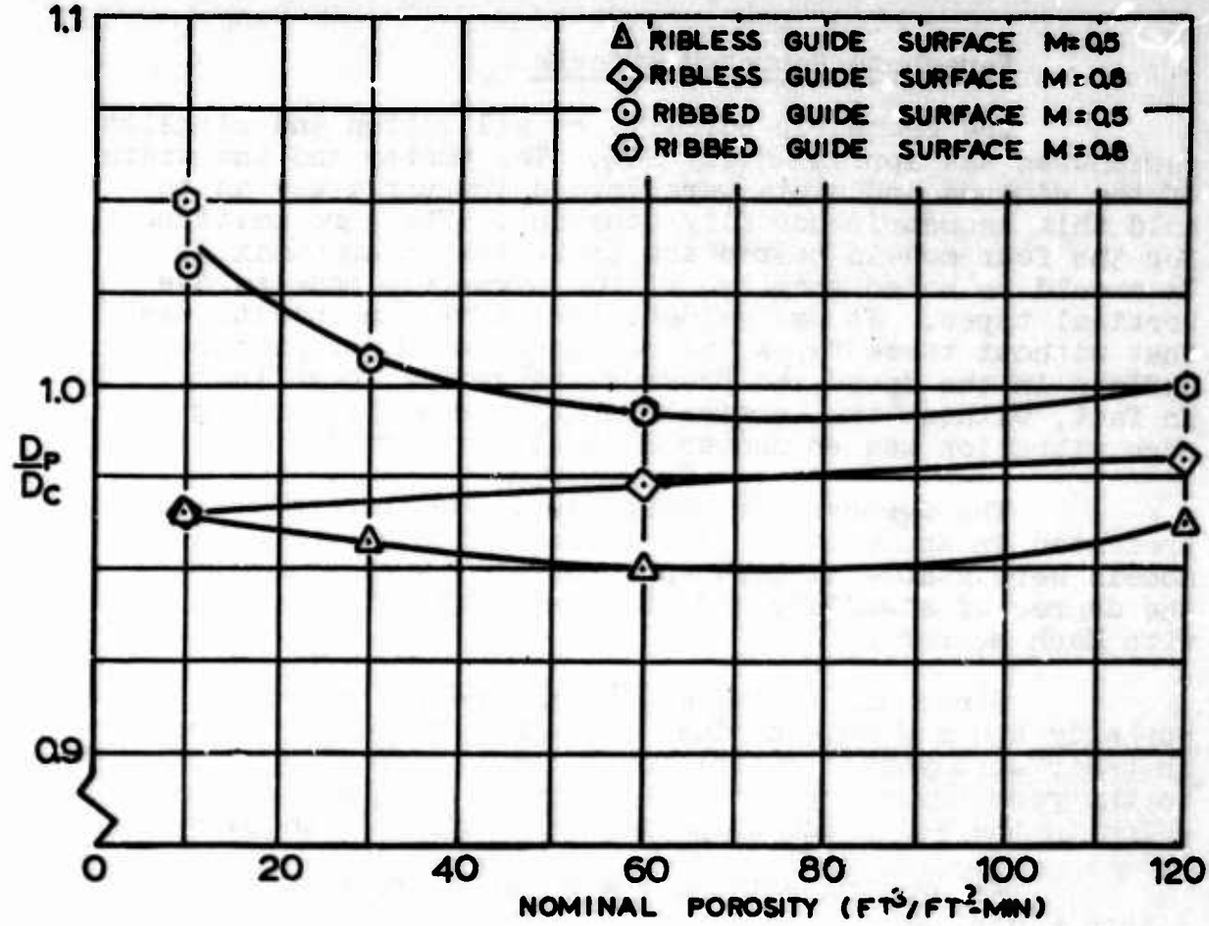


A) Diameter Ratio

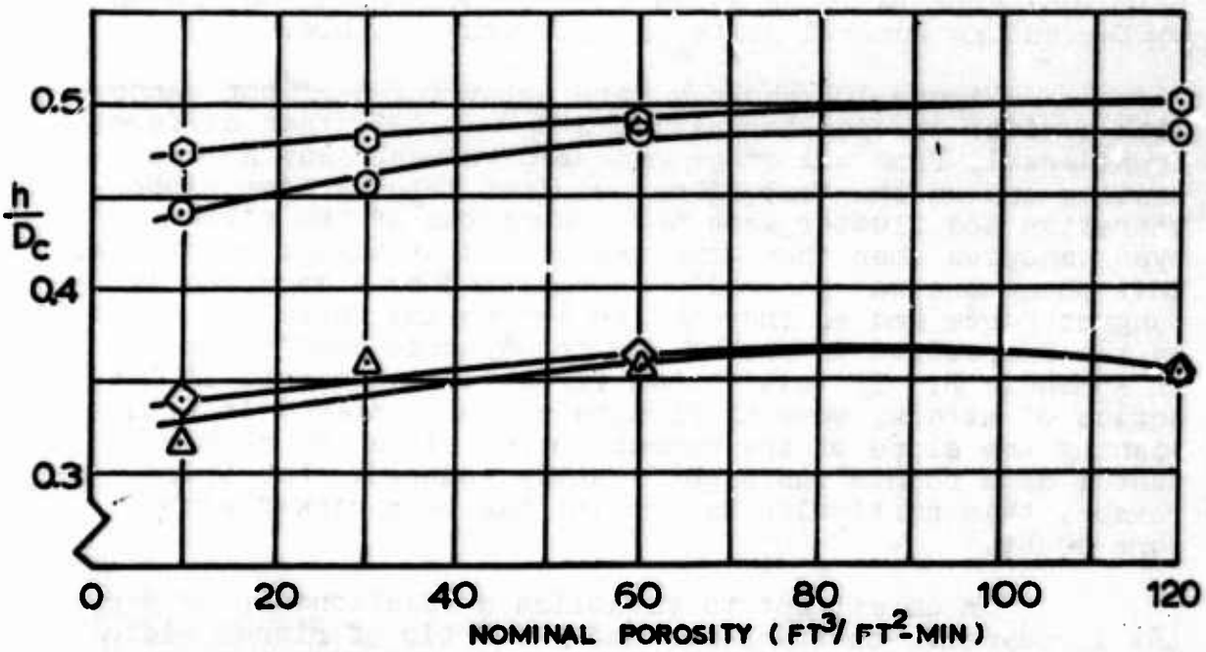


B) Canopy Depth Ratio

Fig 9 Measured In-Flight Dimensions of Ribless and Ribbed Guide Surface Parachutes vs Nominal Porosity

## 3. Parachute Geometry Effects

The geometric porosity of all ribbon and ringslot parachutes was approximately 20%. The number and the width of the ribbons and slots were varied in such a way as to hold this geometric porosity constant. The gore patterns for the four models tested are presented in Appendix A. It should be noted that two ribbon parachute models have vertical tapes. It was evident that after an initial test that without these tapes the canopies would not properly inflate in the speed and pressure ranges of these tests. In fact, without the vertical tapes, excessive leading edge vibration was encountered and several ribbons failed.

The aerodynamic coefficients of these models are presented in Appendix B. The tests indicated that all models were stable at zero angle of attack and that both the degree of stability and the drag efficiency increased with Mach number.

Since all of the models had nearly equal total porosity and the same nominal diameter, the differences in their aerodynamic coefficients can be directly attributed to the geometry changes in the respective gore patterns, which in the end product specify the inflated canopy shape.

Figure 10A relates the drag coefficient to the ribbon width, W, of the canopies. It can be seen that the drag of the canopy increases with the ribbon width in a somewhat linear fashion. The stability derivative $dC_M/d\alpha$ (Fig 10B) appears to be somewhat dependent upon the ribbon width, but no general statement appears possible.

Figure 10B shows a data point for a ribbon canopy with a width to diameter ratio, $W/D_o = 0.039$, that differs considerably from all other measured values. During the testing and on the test films, violent leading edge ribbon vibration and flutter were noticed on two of the ribbon type canopies when they were restrained at angles of attack. This phenomena was generally accompanied by a decrease in tangent force and an increase in the normal force, as noted on the respective graphs of the aerodynamic coefficients in Appendix B. If this ribbon instability occurred at low angles of attack, some difficulty was encountered in establishing the slope of the moment curve, since the number of useful data points was significantly reduced. For this reason, this particular data point has been viewed with some doubt.

In an attempt to establish a relationship between the aerodynamic coefficients and the ratio of ribbon width to free length of the ribbon, the graphs of Fig 11 have been constructed. The free length, f, is the maximum distance between vertical tapes. The tangent force variation

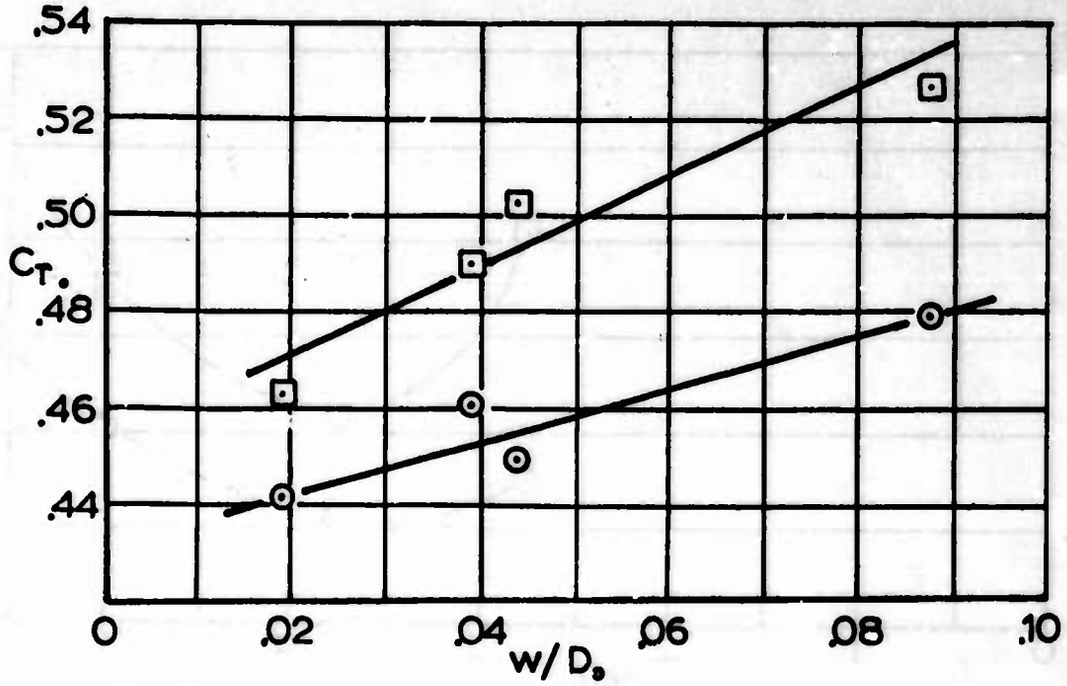


A) Tangent Force

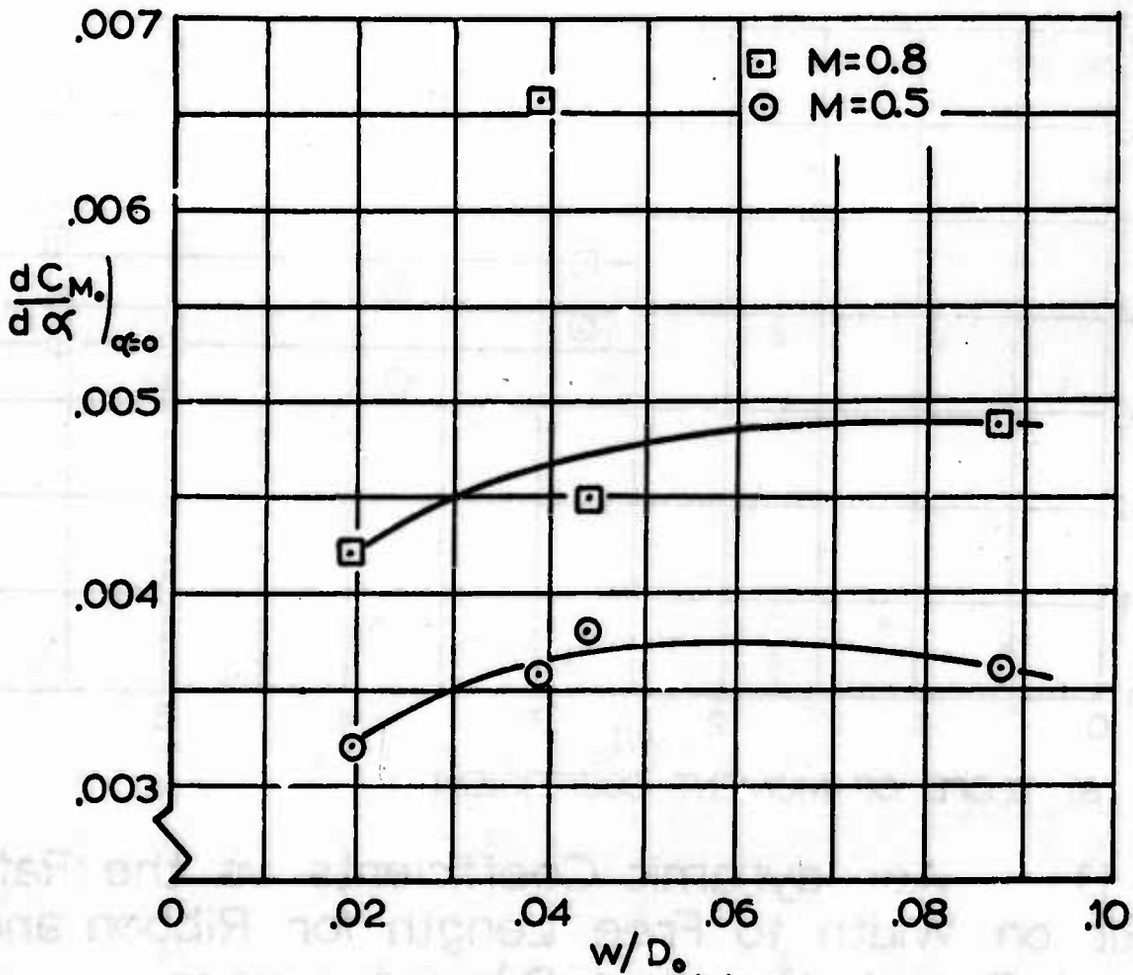


B) Slope of Moment Coefficient

Fig 10 Aerodynamic Coefficient vs the Ratio of Ribbon Width to Nominal Diameter for Ribbon and Ringslot ($\alpha = 0$)

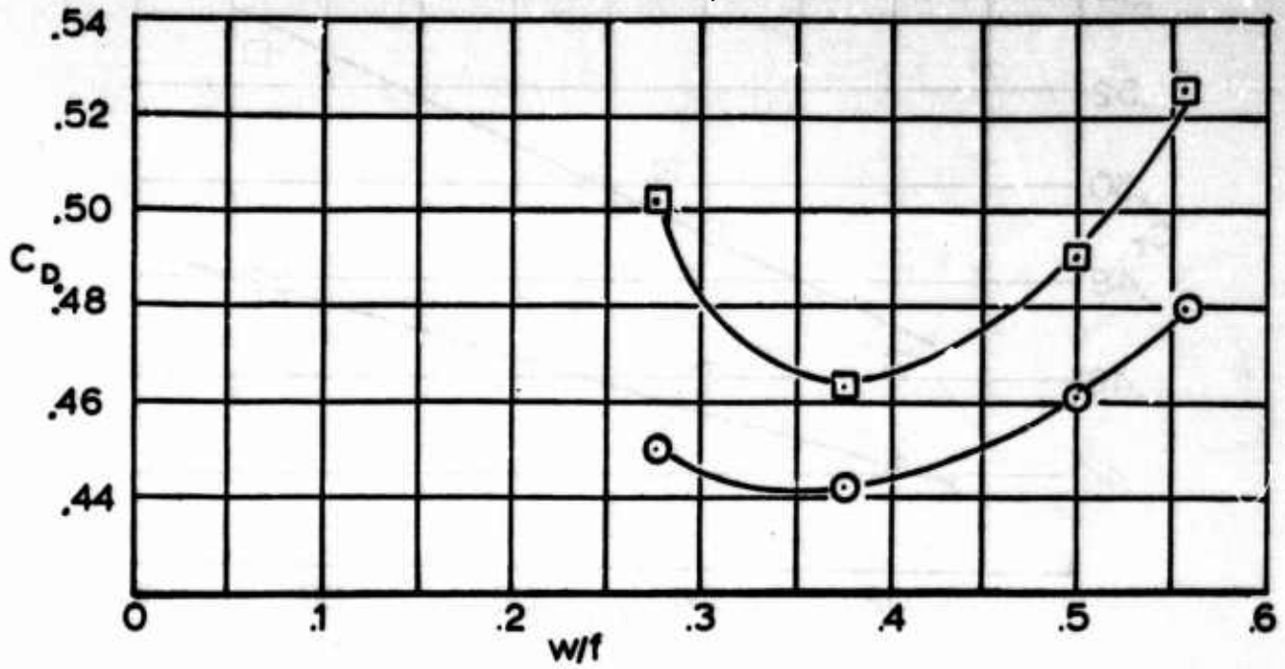


A) TANGENT FORCE

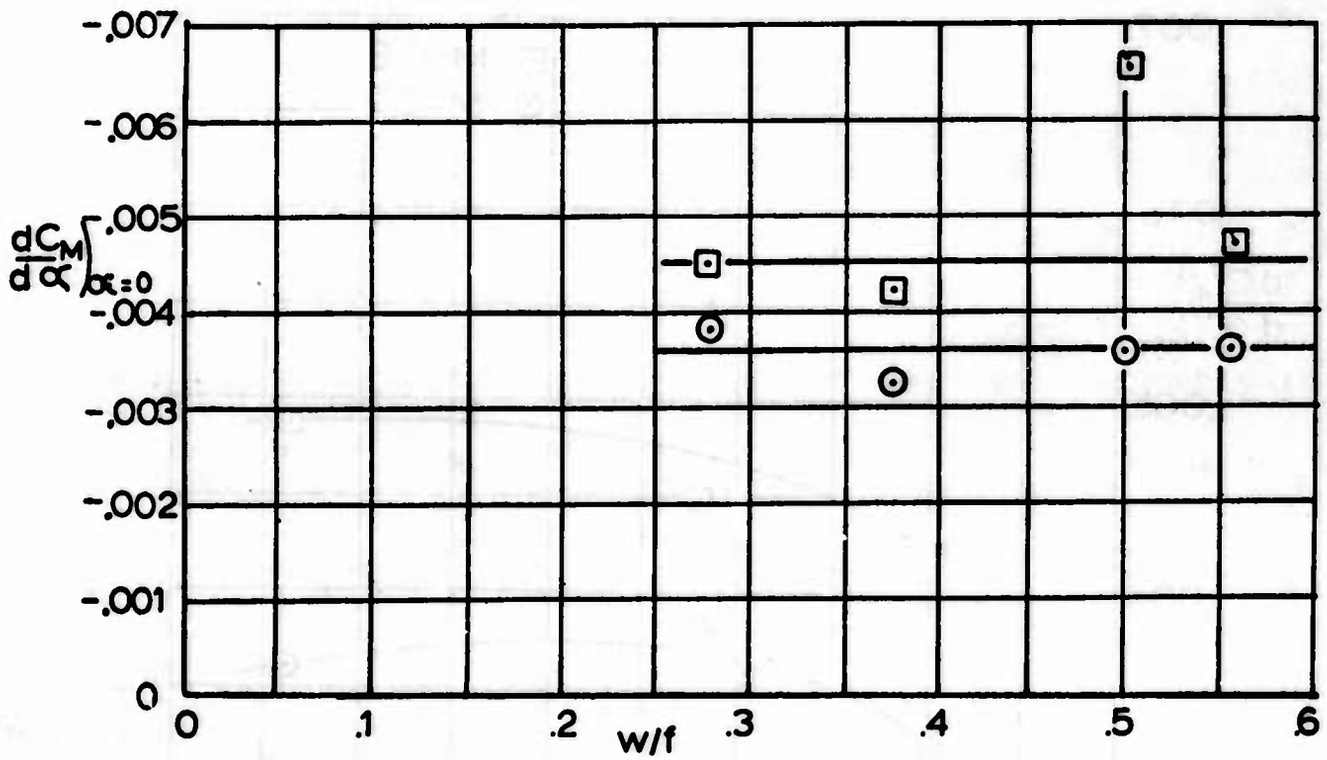


B) SLOPE OF MOMENT COEFFICIENT

Fig 11 Aerodynamic Coefficients vs. the Ratio of Ribbon Width to Free Length for Ribbon and Ringslot Parachutes ($\alpha = 0$)

(Fig 11A) appears somewhat random, and the moment coefficient (Fig 11B) is generally independent of this parameter if the same questionable data point is neglected. As additional information, Table 1 lists the measured profile diameters at the two test Mach number.

TABLE 1

MEASURED PROFILE DIAMETERS AT MACH NUMBERS OF 0.5 AND 0.8 FOR 100" AND 50" RIBBON AND RINGSLOT PARACHUTES

| Parachute Type | $D_p/D_o$ | | $W/D_o$ | W/f |
|---|---|---|---|---|
| | M=0.5 | M=0.8 | | |
| 100" Ribbon | .613 | .613 | .020 | .373 |
| 50" Ribbon | .669 | .675 | .039 | .498 |
| 100" Ringslot | .638 | .656 | .044 | .276 |
| 50" Ringslot | .700 | NA | .068 | .553 |

Nominal Diameter = 16.0"

4. Mach Number Effects

The 50" prototype parachute model, $W/D_o = 0.039$ was selected for further testing to establish the relative differences in the drag coefficient with Mach number changes.

The total pressure for these tests in the Mach number range between 0.5 and 0.9 was held approximately constant in an attempt to rule out any differences due to total pressure or Reynolds number changes. These additional tests were performed at zero angle of attack only, and indicate (Fig 12) a steady increase in the drag coefficient with Mach number throughout the region tested. The canopy performed satisfactorily at all Mach numbers and no excessive ribbon flutter or vibration was noted.

From these tests as well as those included in the main program, it is evident that in general, the drag coefficients of parachutes increase in a fashion similar to those of most other bodies in the transonic flow regime.

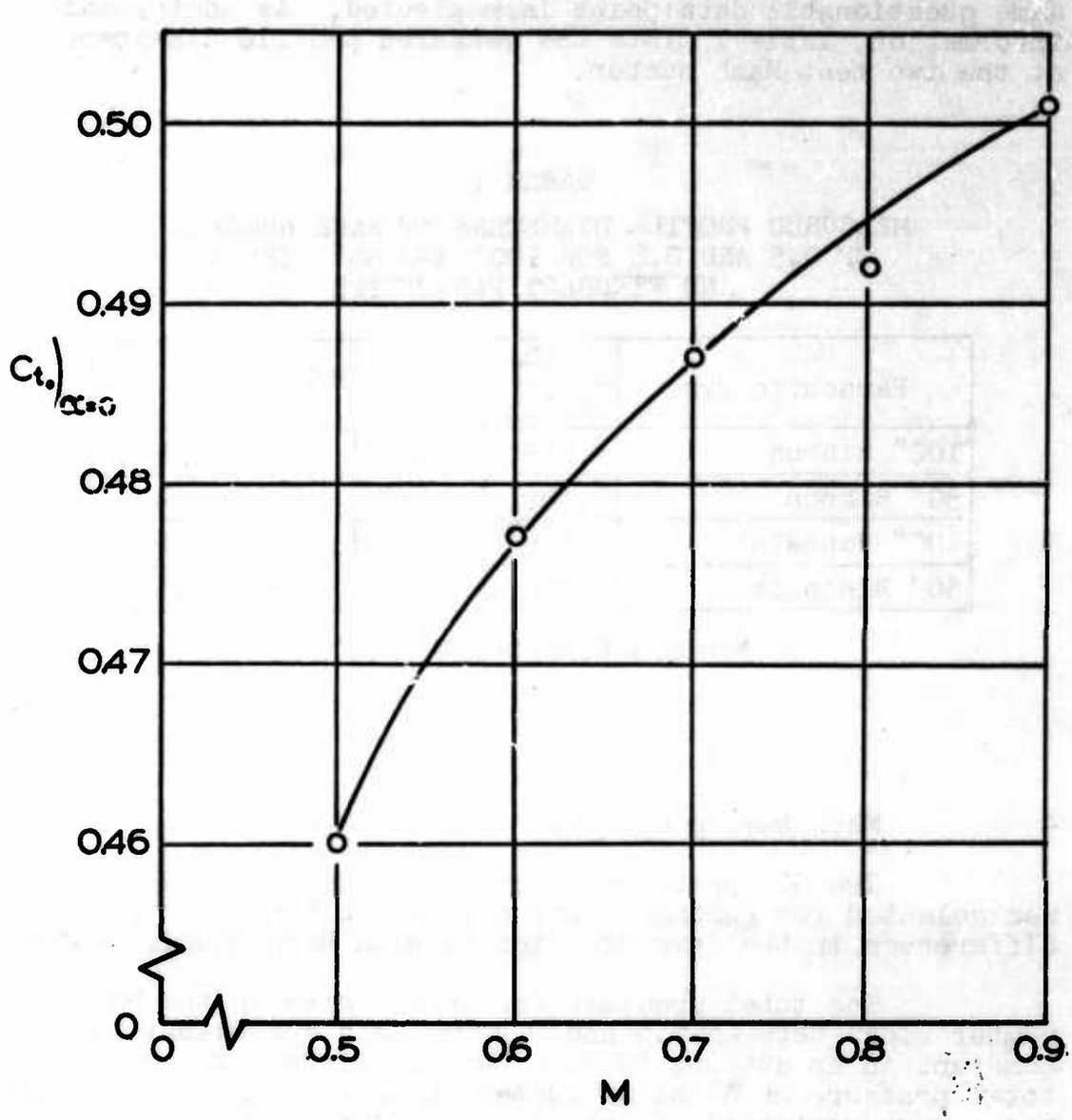


Fig 12 Tangent Force Coefficient as a Function of Mach Number for 50 In. Prototype Ribbon Parachute ($\lambda_g$=20%, W/$D_o$ =0.039)

## IV. SUMMARY

The direct results of the wind tunnel testing shown in Appendix B indicate an increasing tangent force coefficient for all parachutes as Mach number is increased. The moment coefficients and their variation with angle of attack ($dC_M/d\alpha$) seem in general also to increase with increasing Mach number, but the tendency is not a strong one. Experiments also indicate that the aerodynamic coefficients of the guide surface parachutes are dependent upon the effective porosity in the region tested.

Further analysis of this data and additional wind tunnel tests have established several other related facts.

In tests on two guide surface parachutes at a constant Mach number, the tangent force coefficient increased with a total pressure increase, while the moment coefficient remained essentially constant. These tests indicate that although the guide surface canopies remain strongly stable, their drag coefficients may for the same Mach number possible decrease at higher altitude.

From a comparison of the ribbon and ringslot canopy data, there is an indication that for canopies of comparable geometric porosity and the same number of gores, the drag coefficient increases with wider ribbons, while the stability remains unaffected.

Tests on one ribbon parachute model indicate a gradual increase in drag coefficient with Mach number in the range between 0.5 and 0.9 at a constant free stream total pressure, further substantiating the rest results which show a general increase in tangent force coefficient with Mach number.

## V. REFERENCES


1. H. G. Heinrich and E. L. Haak. Stability and Drag of Parachutes with Varying Effective Porosity, ASD-TDR-62-100, Aeronautical Systems Division, Wright-Patterson Air Force Base, Ohio, December, 1961.

2. Performance of and Design Criteria for Deployable Aerodynamic Decelerators, ASD-TR-61-579, Aeronautical Systems Division, Wright-Patterson Air Force Base, Ohio, December, 1963.

3. H. G. Heinrich. Effective Porosity of Parachute Cloth, Zeitschrift fuer Flugwissenschaften, 11 (1963), Heft 10, Braunschweig.

## APPENDIX A

## CANOPY GORE PATTERNS AND STRENGTH TESTS

### 1. Gore Patterns

The parachutes tested in this program are the following:

a) ribless guide surface, 4 porosities

b) ribbed guide surface, 4 porosities

c) ribbon, 18% porosity, 2 ribbon widths

d) ringslot, 20% porosity, 2 ribbon widths

General specifications for construction of these parachutes are presented in Ref 2. Specific dimensions for the canopies are presented in Figs 13 through 16, and in Table 2.

### 2. Strength Tests

Parachutes tested at high subsonic speeds are subjected to high dynamic pressures, and therefore, high stress loadings. Particular areas of stress concentration are at the confluence point of the suspension lines, and along the canopy seams. Calculations at M = 0.8 (assuming sea level stagnation density) yields a maximum dynamic pressure of approximately 600 lbs/ft$^2$. This dynamic pressure predicts a stress of 40 lbs/in. along the seams of a ribbed guide surface canopy, and a load of 600 lbs on the confluence point. Tests were performed to determine whether the models could withstand these loadings. Results are summarized in two parts:

A. Confluence Point and Suspension Lines

To maintain minimum interference, the confluence region was kept small in cross-sectional area. After several arrangements had been tested, the final confluence point configuration, shown earlier in Fig 2A, was established. With this arrangement, the suspension lines are capable of withstanding loads in excess of 1,000 lbs, as verified in experimental testing.

The suspension line design consists of continuous lines (Fig 17) sewn along the seams of the parachute canopy.

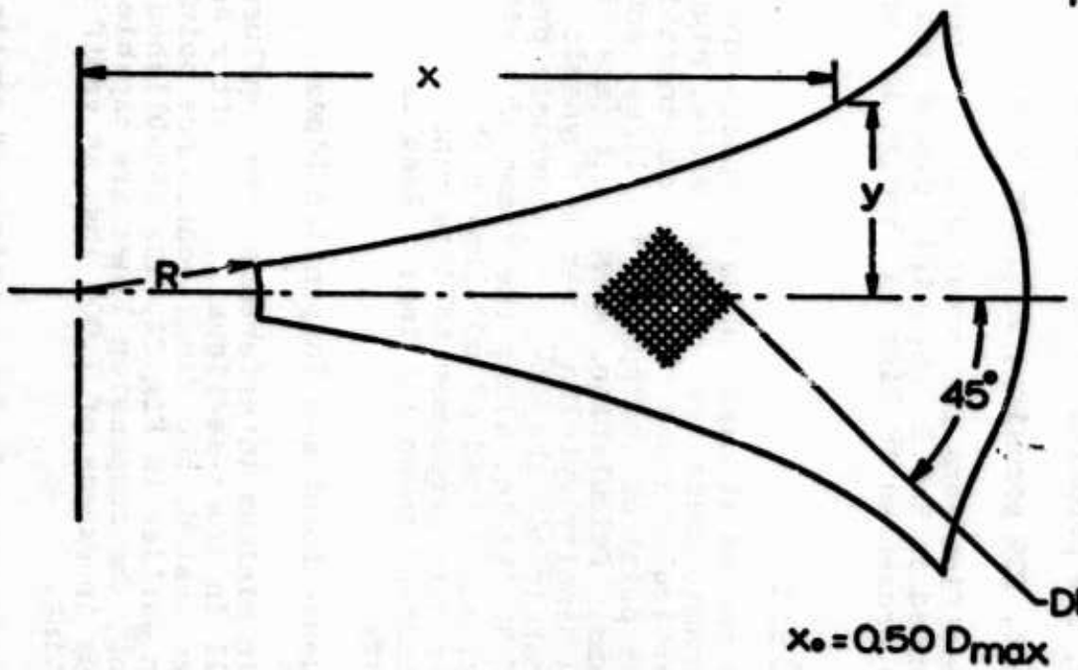


NOTE: a) THE PARACHUTE HAS 12 PANELS

b) THE PATTERN DIMENSIONS DO NOT INCLUDE SEAM ALLOWANCE

c) MATERIAL:

d) SUSPENSION LINE LENGTH = 168 in WITH 25 lb LOAD PER LINE

| $x/x_o$ | 0.10 | 0.15 | 0.20 | 0.30 | 0.40 | 0.50 | 0.60 | 0.70 | 0.80 | 0.875 | 0.90 | 0.95 | 0.975 | 1.0 |
|---|---|---|---|---|---|---|---|---|---|---|---|---|---|---|
| $y/x$ | 0.394 | 0.394 | 0.394 | 0.407 | 0.410 | 0.416 | 0.428 | 0.441 | 0.495 | 0.676 | 0.527 | 0.261 | 0.1625 | 0.0 |

Fig 13 Roof Pattern for Ribless Guide Surface Parachute

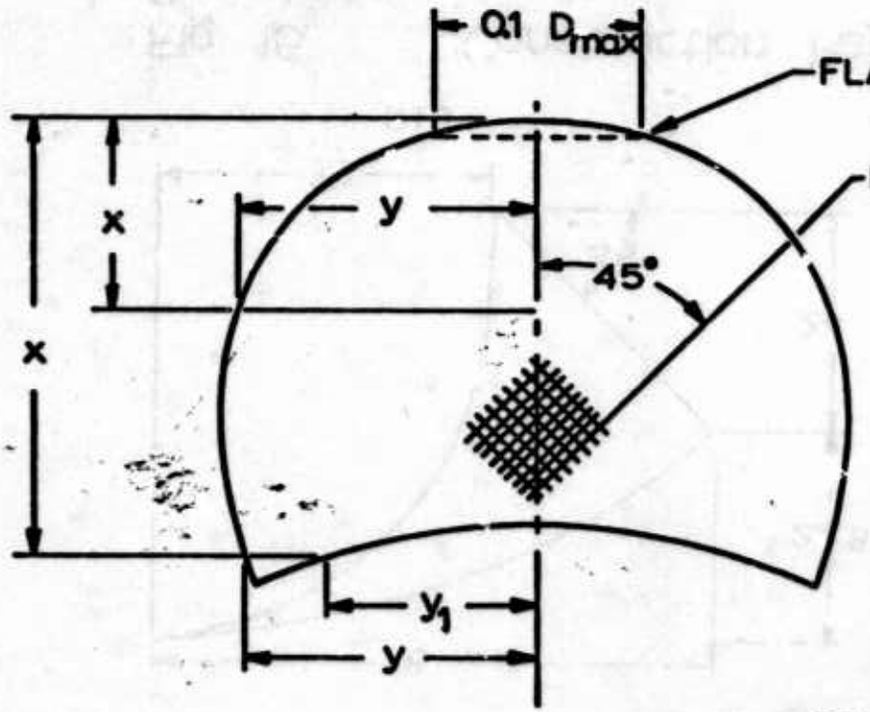


NOTE: a) THE PARACHUTE HAS 12 PANELS
b) THE PATTERN DIMENSIONS DO NOT INCLUDE SEAM ALLOWANCE
c) MATERIAL:
d) ONE SLOT IN EACH PANEL 0.1 $D_{max}$ WIDE

$x_o = 0.23\ D_{max}$

| $x/x_o$ | 0.05 | 0.10 | 0.15 | 0.20 | 0.30 | 0.40 | 0.50 | 0.60 | 0.70 | 0.80 | 0.90 | 0.93 | 0.95 | 1.00 |
|---|---|---|---|---|---|---|---|---|---|---|---|---|---|---|
| $y/x$ | 4.33 | 3.21 | 2.58 | 2.13 | 1.58 | 1.25 | 1.03 | 0.86 | 0.722 | 0.61 | 0.515 | 0.491<br>0.000 | 0.472<br>0.226 | 0.430 |

Fig 14 Guide Surface Pattern for Ribless Guide Surface Parachute.

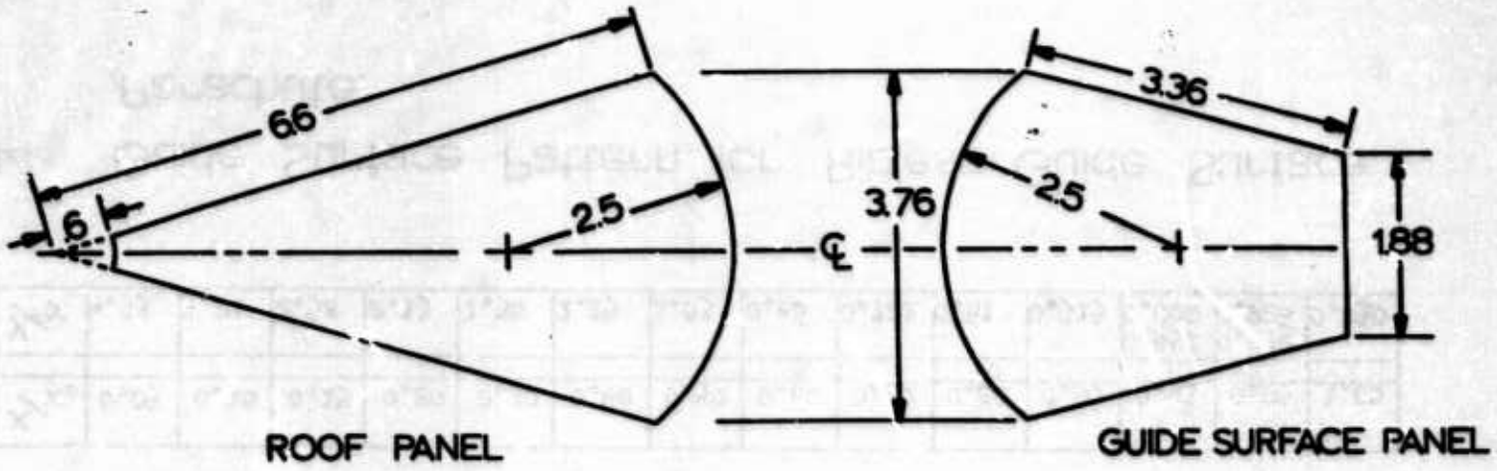


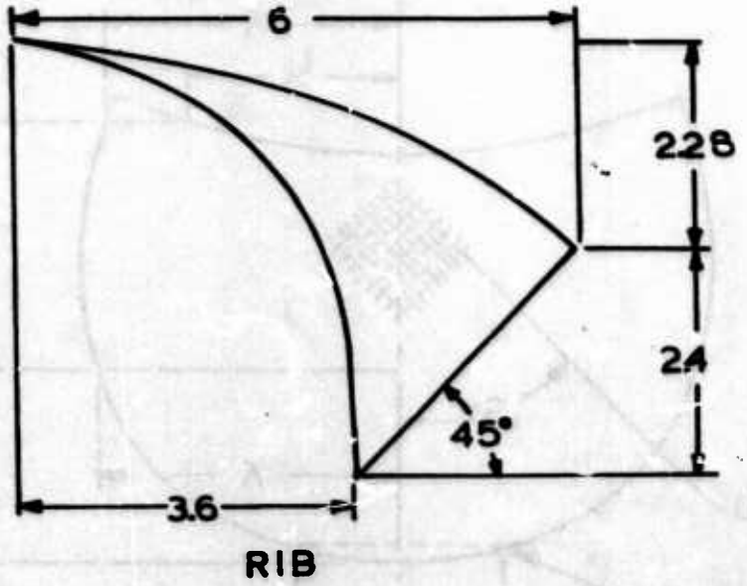


DIMENSIONS IN INCHES
$D_e$ = 12 in., 12 GORES

SUSPENSION LINE LENGTH
= 16 in. WITH 25 lb. LOAD
PER LINE

Fig 15. Construction Patterns for Ribbed Guide Surface Parachute

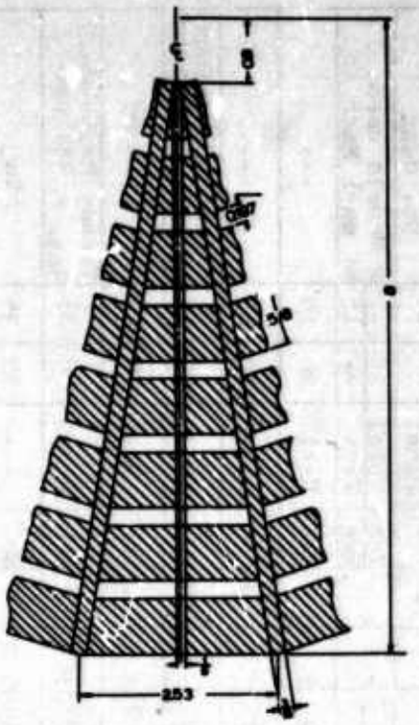


RIBBON, 50 in. PROTOTYPE

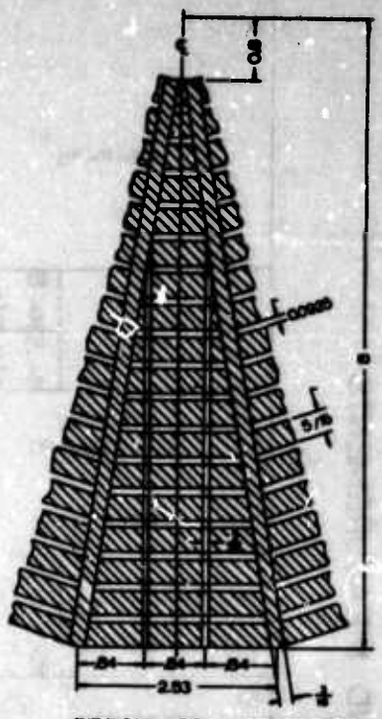


RIBBON, 100 in. PROTOTYPE

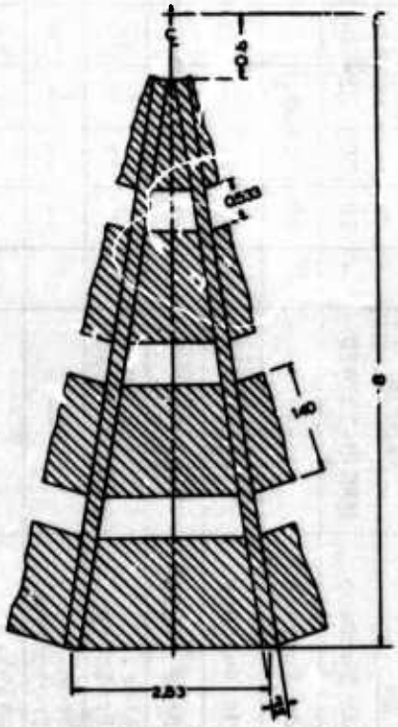


RINGSLOT, 50 in. PROTOTYPE

SUSPENSION LINE LENGTH = 16.0 in. UNDER 15 lb. TENSION PER LINE

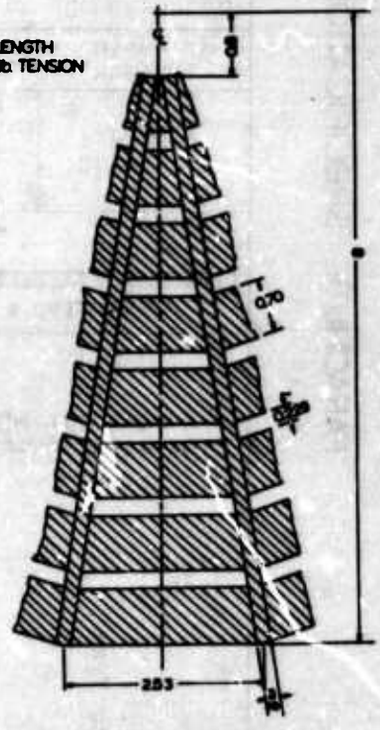


RINGSLOT, 100 in. PROTOTYPE

Fig 16. Gore Patterns for Circular Flat Ribbon and Ringslot Parachutes ($D_o$ = 16 in, 20 GORES)

# TABLE 2

## PARACHUTE SPECIFICATIONS AND MEASUREMENTS

| Parachute Type | Canopy Material Specifications | % Calculated Geometric Porosity | Nominal Porosity $\frac{ft^3}{ft^2 min}$ | Effective Porosity C M=.5 | Effective Porosity C M=.8 | Nominal Diameter $D_o$ in. | Constructed Diameter $D_c$ in. | Ribbon Width Ratios $\frac{w}{D_o}$ | Ribbon Width Ratios $\frac{W}{f}$ | Canopy Depth from Photographs M=.5 h in. | Canopy Depth from Photographs M=.8 h in. | Test Damage | Location of Failure | Test Time M=.5 min. | Test Time M=.8 min. | Remarks |
|---|---|---|---|---|---|---|---|---|---|---|---|---|---|---|---|---|
| Ribless Guide Surface | MIL-M-10747D | -- | 10 | .003 | .004 | -- | 12.6 | -- | -- | 4.0 | 4.3 | No | --- | 30 | 25 | --- |
| Ribless Guide Surface | --- | -- | 30 | .014 | .011 | -- | 12.6 | -- | -- | 4.6 | -- | Yes | Guide Panels | 25 | -- | No Test, M=0.8 |
| Ribless Guide Surface | MIL-C-8021A Type I | -- | 60 | .019 | .017 | -- | 12.6 | -- | -- | 4.5 | 4.6 | Yes | Vent Area | 20 | 10 | --- |
| Ribless Guide Surface | MIL-C-7020B Type I | -- | 120 | .049 | .042 | -- | 12.6 | -- | -- | 4.5 | 4.5 | Yes | Guide Panel | 65 | 15 | Tested at Various po, qmax |
| Ribbed Guide Surface | MIL-M-10747D | -- | 10 | .003 | .004 | -- | 12.0 | -- | -- | 5.3 | 5.7 | Yes | Total | 25 | -- | 2 Models used, 1 at each Mach no. |
| | | | | | | | | | | | | Yes | Vent | -- | 15 | |
| Ribbed Guide Surface | --- | -- | 30 | .014 | .011 | -- | 12.0 | -- | -- | 5.5 | 5.8 | Yes | Vent | 20 | 10 | --- |
| Ribbed Guide Surface | MIL-C-8021A Type I | -- | 60 | .019 | .017 | -- | 12.0 | -- | -- | 5.8 | 5.9 | No | --- | 110 | 15 | --- |
| Ribbed Guide Surface | MIL-C-7020B Type I | -- | 120 | .049 | .042 | -- | 12.0 | -- | -- | 5.8 | 6.0 | Yes | Panel | 20 | 15 | Tested at Various po, qmax = 270 psf |
| Ribbon, 50 in. Prototype | 5/8 in. Tape Class B, Type 3 | 18 | -- | -- | -- | 16 | -- | .039 | .498 | 4.6 | 4.7 | No | --- | 30 | 20 | --- |
| Ribbon, 100 in. Prototype | --- | 18 | -- | -- | -- | 16 | -- | .020 | .373 | 4.8 | 4.8 | No | --- | 40 | 35 | Tested M=.5→M=.9 qmax = 334 psf |
| Ringslot, 50 in. Prototype | --- | 20 | -- | -- | -- | 16 | -- | .088 | .553 | 5.3 | 5.3 | No | --- | 30 | 35 | --- |
| Ringslot, 100 in. Prototype | --- | 20 | -- | -- | -- | 16 | -- | .044 | .276 | 4.8 | 4.8 | No | --- | 35 | 20 | --- |

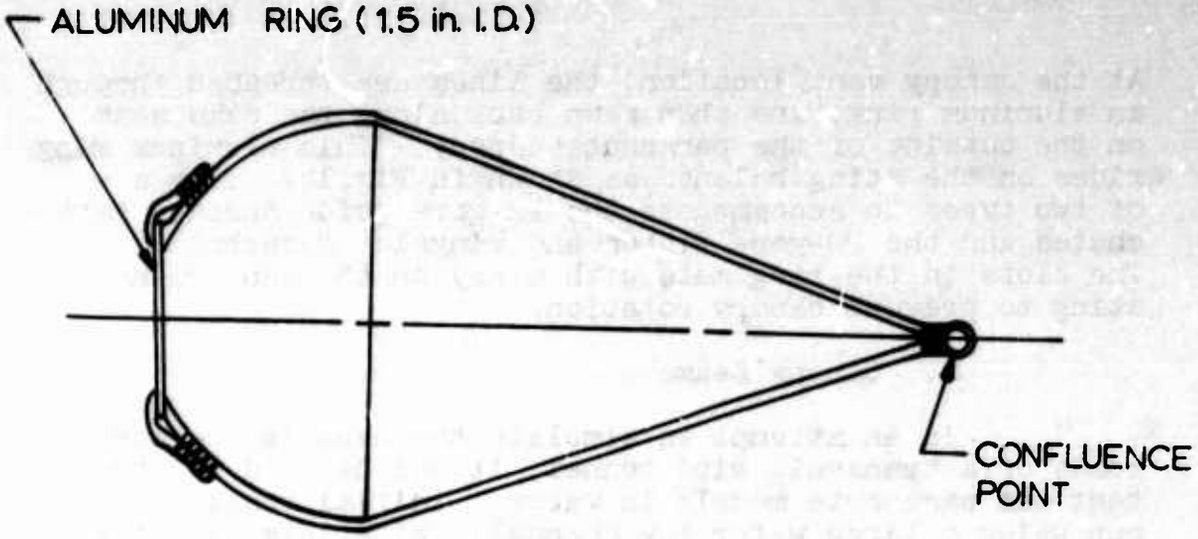


Fig 17. Suspension Line System

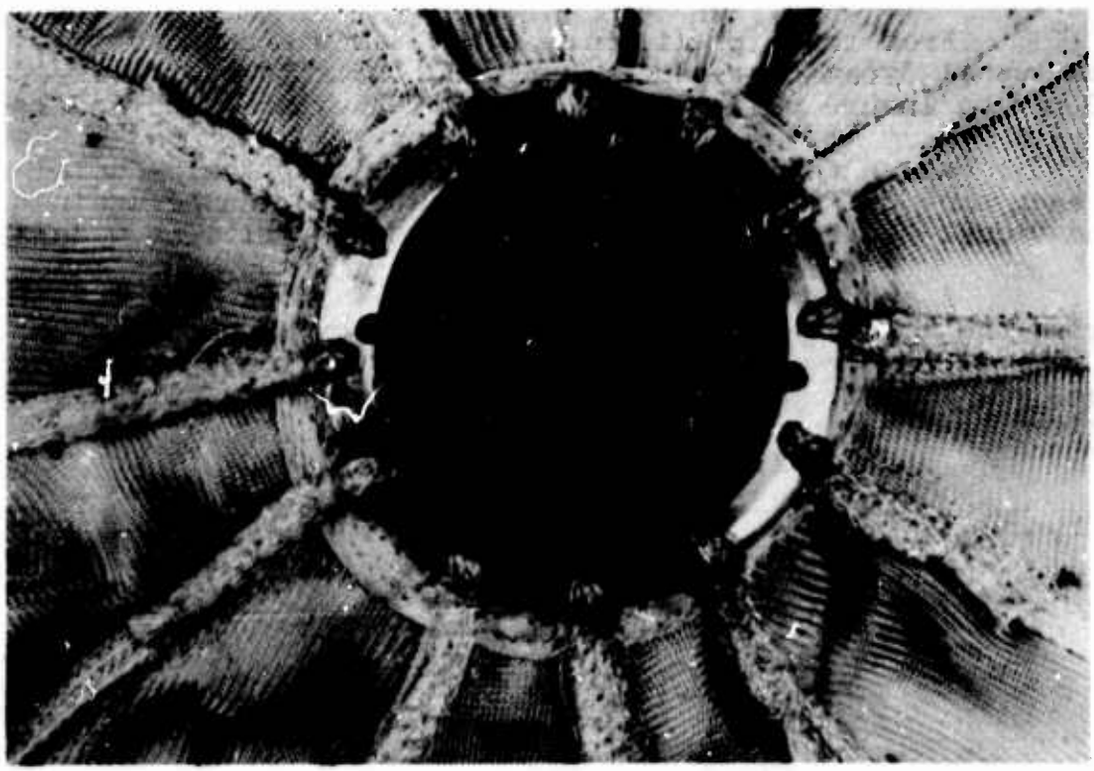

Fig 18. Canopy Vent Ring

At the canopy vent location, the lines are threaded through an aluminum ring, and then sewn back along the same seam on the outside of the parachute canopy. This aluminum ring rides on the sting balance as shown in Fig 18. They are of two types to accommodate the 12-gore guide surface parachutes and the 20-gore ribbon and ringslot parachutes. The slots in the ring mate with a key on the center-line sting to prevent canopy rotation.

B. Canopy Seams

In an attempt to simulate the dynamic pressure loads of a transonic wind tunnel, it was decided to strength test the parachute models in water. Initial tests were run using a large water tow channel. With this facility, dynamic pressures of 120 psf were obtained without damage to the canopy.

Further tests behind a motor boat produced failure of ribless guide surface canopies constructed of 40 lb and 90 lb cloth. Although highly accurate determination of failure loadings was impossible, estimates place the magnitude of dynamic pressure at failure between 300 psf and 400 psf.

From these preliminary tests, it was decided that wind tunnel dynamic pressure should not be allowed to exceed 300 psf to insure reliable operation of the parachute models.

As an additional safeguard, two identical models of each test configuration were fabricated to insure against wind tunnel shutdown caused by the lack of sufficient models.

A summary of the damage to the various canopies during the actual wind tunnel running is contained in Table 2. In general, the models performed well and the damage in most cases was slight. When damage did occur it was usually limited to the vent area.

# APPENDIX B

## AERODYNAMIC COEFFICIENTS OF PARACHUTES

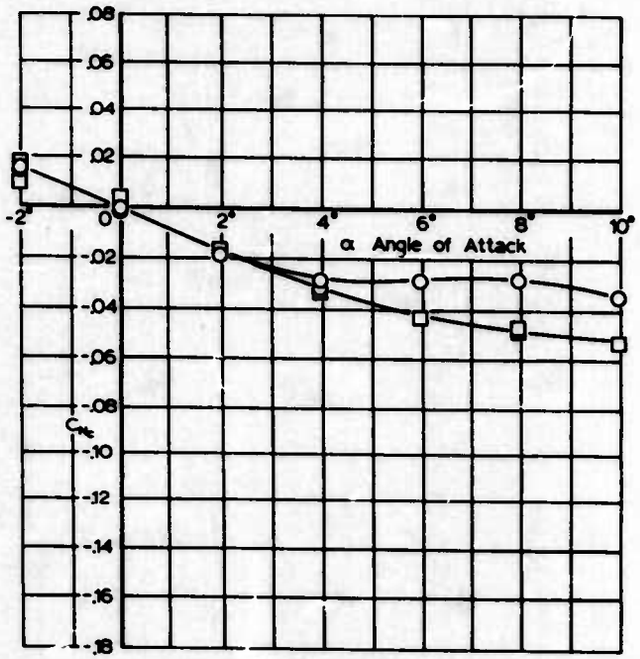


NORMAL FORCE COEFFICIENT

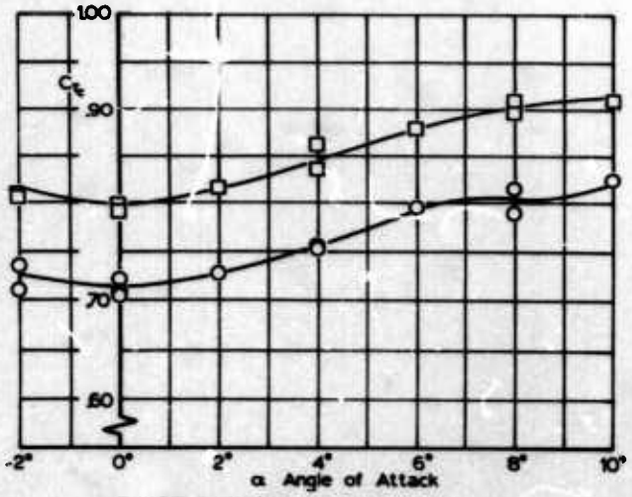


TANGENT FORCE COEFFICIENT

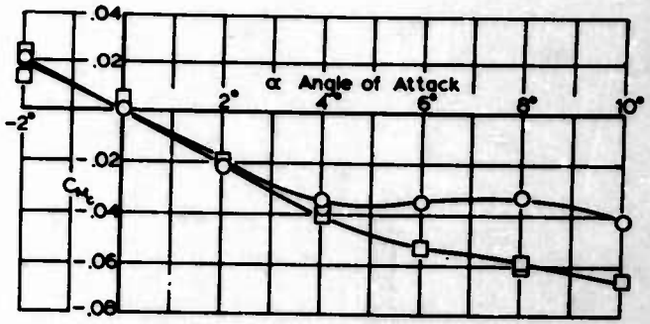


MOMENT COEFFICIENT

○ M=0.5 Re = 1.3 x $10^6$
□ M=0.8 Re = 1.9 x $10^6$

Fig 19. Aerodynamic Coefficients vs. Angle of Attack for Ribless Guide Surface Parachute (Nominal Porosity = 10 $ft^3/ft^2$ min)

TABLE 3

AERODYNAMIC COEFFICIENTS FOR RIBLESS GUIDE SURFACE PARACHUTE
BASED ON CONSTRUCTION AREA, $S_c$ (NOMINAL POROSITY = 10 $ft^3/ft^2$-min)

| $\alpha$ | 0 | ±2 | ±4 | +6 | +8 | +10 |
|---|---|---|---|---|---|---|
| $C_M$ | .0 | ∓0.020 | ∓0.033 | -0.035 | -0.035 | -0.042 |
| $C_N$ | .0 | ∓0.016 | ∓0.027 | -0.028 | -0.027 | -0.034 |
| $C_T$ | 0.713 | 0.775 | 0.754 | 0.795 | 0.803 | 0.825 |

M=0.5

| $\alpha$ | 0 | ±2 | ±4 | +6 | +8 | +10 |
|---|---|---|---|---|---|---|
| $C_M$ | .0 | ∓0.020 | ∓0.039 | -0.056 | -0.063 | -0.070 |
| $C_N$ | .0 | ∓0.016 | ∓0.031 | -0.041 | -0.048 | -0.052 |
| $C_T$ | 0.795 | 0.812 | 0.847 | 0.879 | 0.905 | 0.910 |

M=0.8

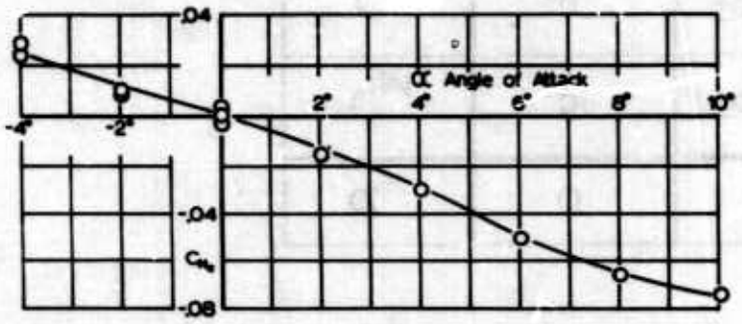


NORMAL FORCE COEFFICIENT

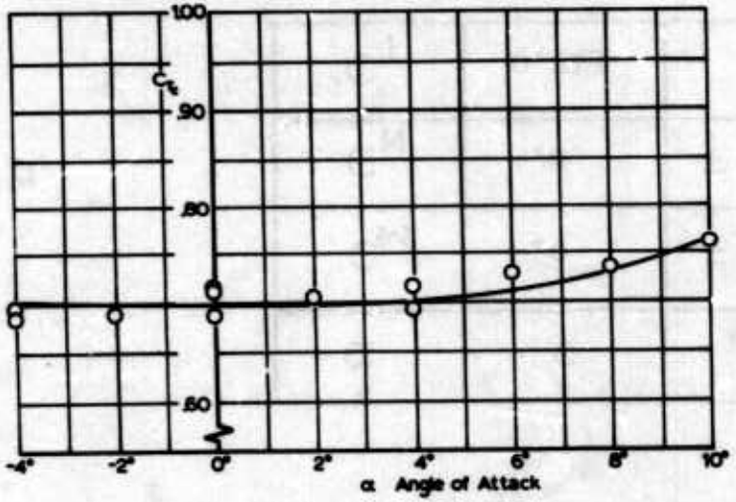


TANGENT FORCE COEFFICIENT

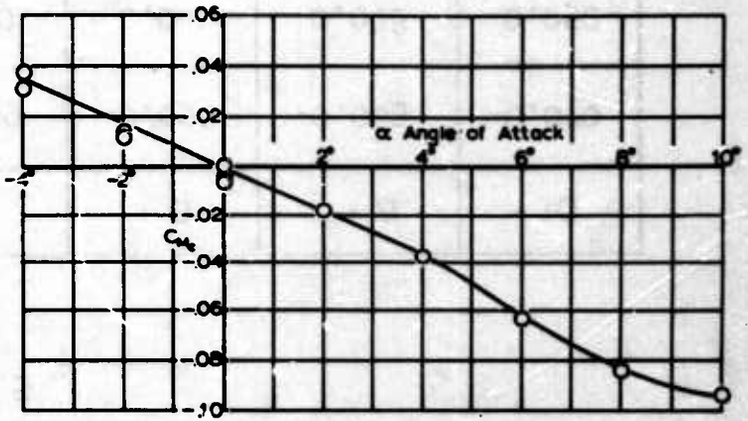


MOMENT COEFFICIENT

O M=0.5 Re = $1.3 \times 10^6$

Fig 20. Aerodynamic Coefficients vs. Angle of Attack for Ribless Guide Surface Parachute (Nominal Porosity = 30 $ft^3/ft^2$ min)

TABLE 4

AERODYNAMIC COEFFICIENTS FOR RIBLESS GUIDE SURFACE PARACHUTE BASED ON CONSTRUCTION AREA, $S_c$ (NOMINAL POROSITY = 30 $ft^3/ft^2$-min)

| $\alpha$ | 0 | ±2 | ±4 | ±6 | ±8 | ±10 |
|---|---|---|---|---|---|---|
| $C_M$ | .0 | ∓0.016 | ∓0.037 | -0.064 | -0.084 | -0.094 |
| $C_N$ | .0 | ∓0.013 | ∓0.029 | -0.050 | -0.066 | -0.074 |
| $C_T$ | 0.710 | 0.697 | 0.704 | 0.729 | 0.744 | 0.762 |

M=0.5

| $\alpha$ | 0 | ±2 | ±4 | ±6 | ±8 | ±10 |
|---|---|---|---|---|---|---|
| $C_M$ | | | | | | |
| $C_N$ | | | | | | |
| $C_T$ | | | | | | |

M=0.8

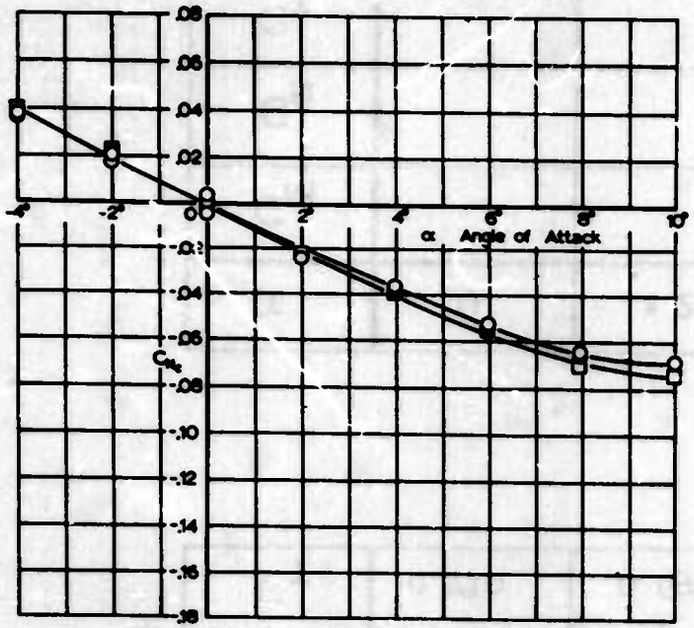


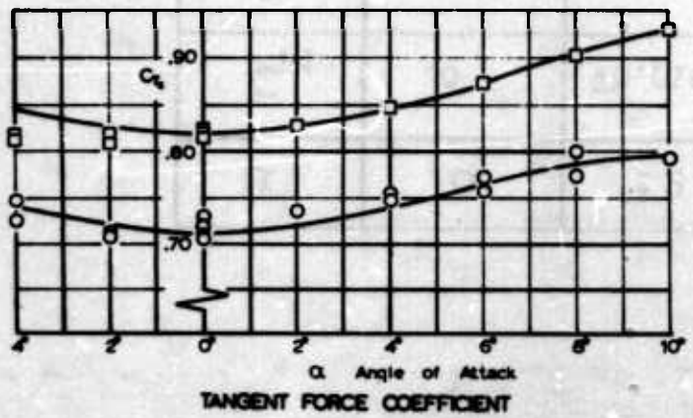


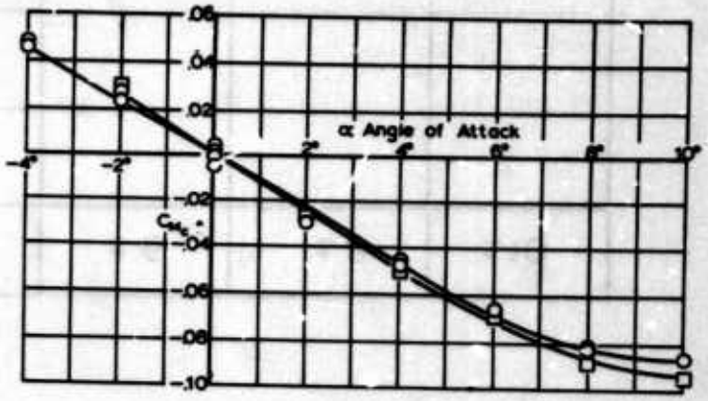


○ M=0.5 Re = 1.3 x $10^6$
□ M=0.8 Re = 1.9 x $10^6$

Fig 21. Aerodynamic Coefficients vs. Angle of Attack for Ribless Guide Surface Parachute (Nominal Porosity = 60 $ft^3/ft^2$ min)

TABLE 5

AERODYNAMIC COEFFICIENTS FOR RIBLESS GUIDE SURFACE PARACHUTE BASED ON CONSTRUCTION AREA, $S_c$ (NOMINAL POROSITY = 60 $ft^3/ft^2$-min)

| $\alpha$ | 0 | ±2 | ±4 | ±6 | ±8 | ±10 |
|---|---|---|---|---|---|---|
| $C_M$ | .0 | ∓0.025 | ∓0.051 | -0.072 | -0.082 | -0.088 |
| $C_N$ | .0 | ∓0.020 | ∓0.040 | -0.053 | -0.065 | -0.069 |
| $C_T$ | 0.722 | 0.723 | 0.746 | 0.766 | 0.787 | 0.792 |

M = 0.5

| $\alpha$ | 0 | ±2 | ±4 | ±6 | ±8 | ±10 |
|---|---|---|---|---|---|---|
| $C_M$ | .0 | ∓0.024 | ∓0.046 | -0.073 | -0.088 | -0.094 |
| $C_N$ | .0 | ∓0.019 | ∓0.036 | -0.058 | -0.069 | -0.074 |
| $C_T$ | 0.821 | 0.821 | 0.832 | 0.873 | 0.903 | 0.931 |

M = 0.8

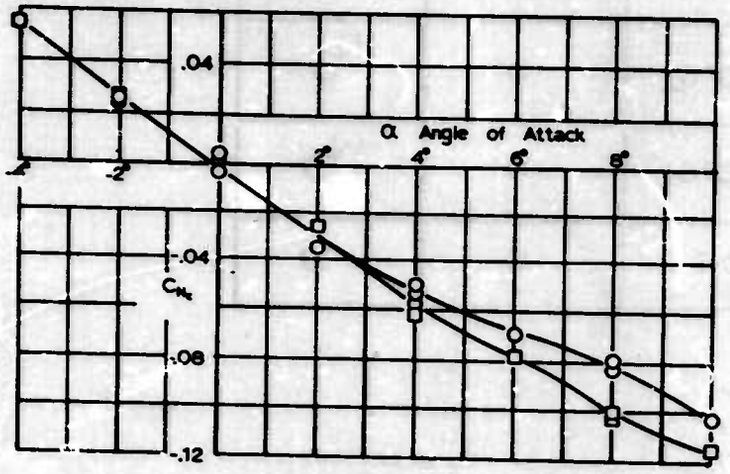


NORMAL FORCE COEFFICIENT

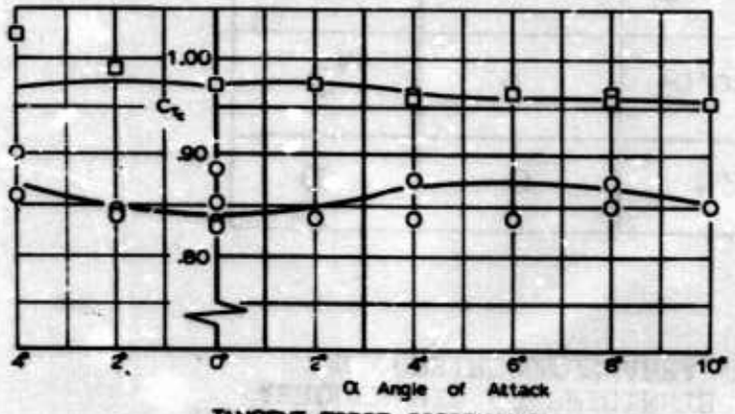


TANGENT FORCE COEFFICIENT

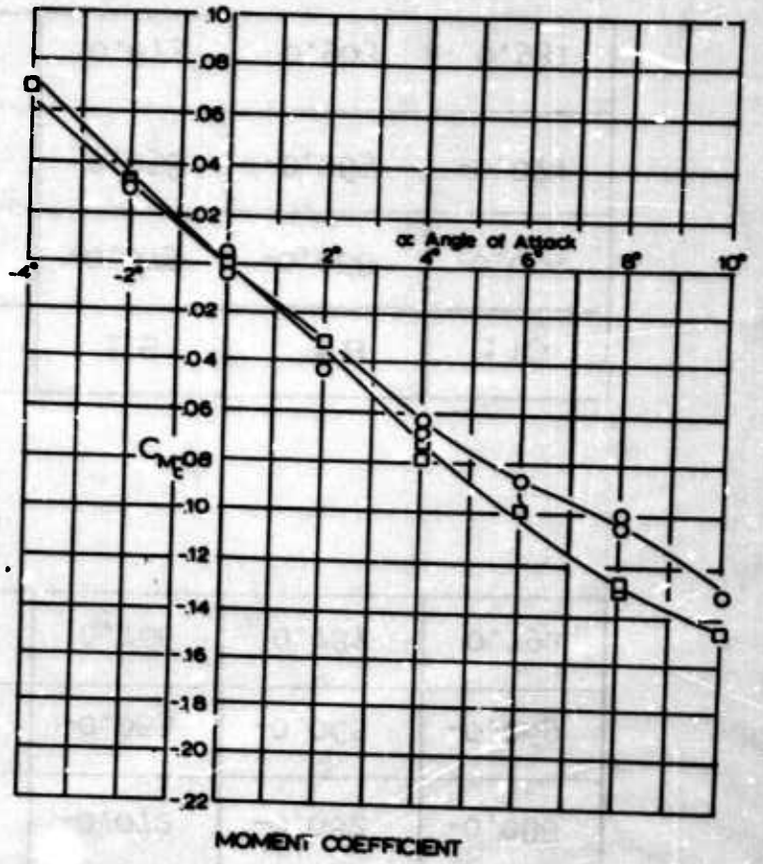


MOMENT COEFFICIENT

○ M=0.5 Re = 1.3 x $10^6$
□ M=0.8 Re = 1.9 x $10^6$

Fig 22. Aerodynamic Coefficients vs. Angle of Attack for Ribless Guide Surface Parachute ( Nominal Porosity = 120 $ft^3/ft^2$ min )

TABLE 6

AERODYNAMIC COEFFICIENTS FOR RIBLESS GUIDE SURFACE PARACHUTE BASED ON CONSTRUCTION AREA, $S_c$ (NOMINAL POROSITY = 120 $ft^3/ft^2$-min)

| $\alpha$ | 0 | ±2 | ±4 | ±6 | ±8 | ±10 |
|---|---|---|---|---|---|---|
| $C_M$ | .0 | ∓0.038 | ∓0.065 | -0.086 | -0.103 | -0.129 |
| $C_N$ | .0 | ∓0.030 | ∓0.052 | -0.068 | -0.081 | -0.102 |
| $C_T$ | 0.851 | 0.841 | 0.869 | 0.839 | 0.860 | 0.850 |

M = 0.5

| $\alpha$ | 0 | ±2 | ±4 | ±6 | ±8 | ±10 |
|---|---|---|---|---|---|---|
| $C_M$ | .0 | ∓0.038 | ∓0.073 | -0.109 | -0.126 | -0.146 |
| $C_N$ | .0 | ∓0.030 | ∓0.058 | -0.078 | -0.100 | -0.115 |
| $C_T$ | 0.973 | 0.974 | 0.994 | 0.966 | 0.962 | 0.956 |

M = 0.8

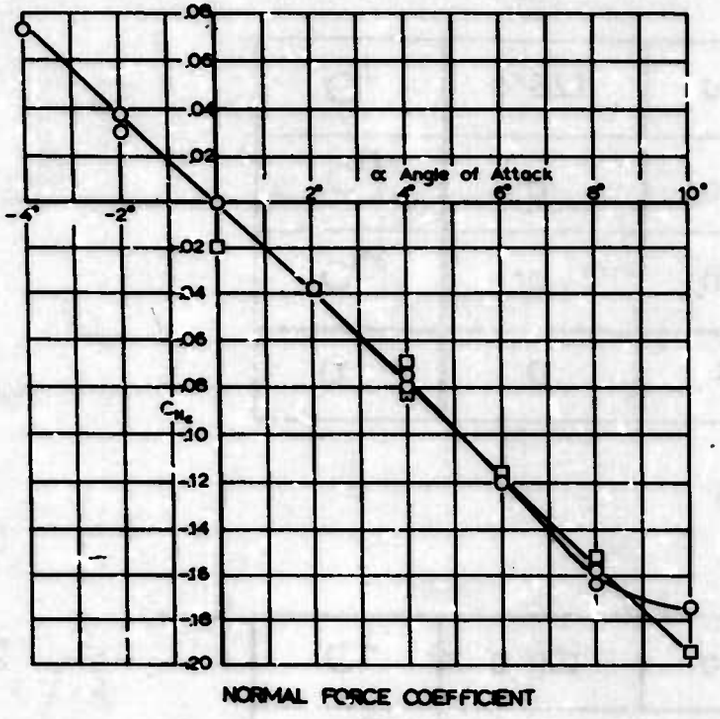


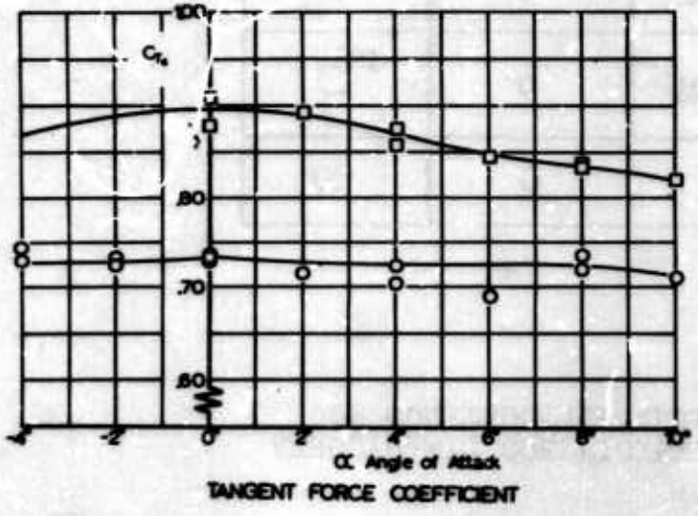


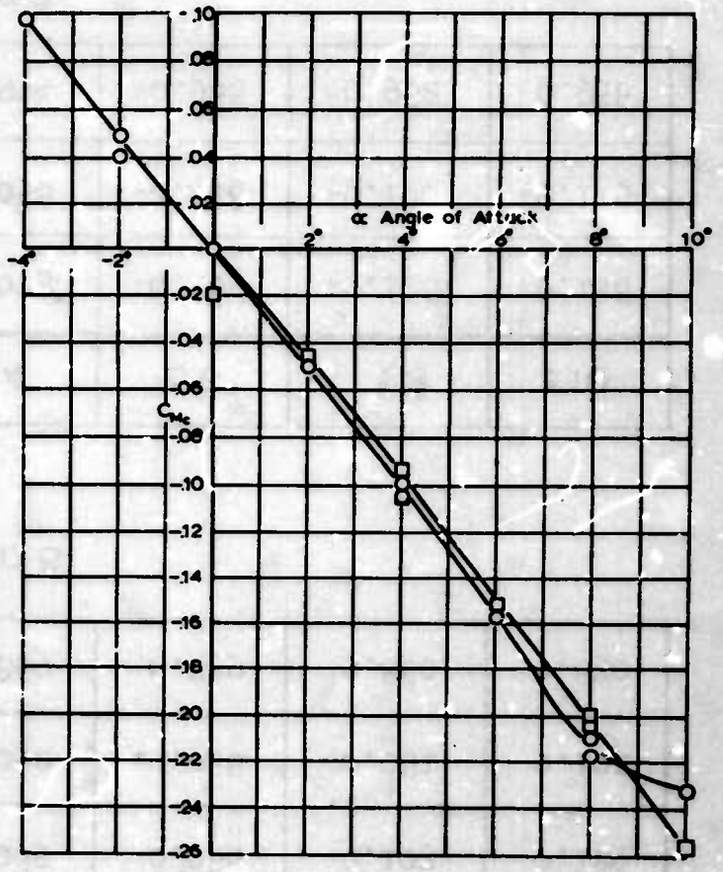


○ M=0.5 Re = 1.3 x $10^6$
□ M=0.8 Re = 1.9 x $10^6$

Fig 23. Aerodynamic Coefficients vs. Angle of Attack for Ribbed Guide Surface Parachute ( Nominal Porosity = 10 $ft^3/ft^2$ min )

TABLE 7

AERODYNAMIC COEFFICIENTS FOR RIBBED GUIDE SURFACE PARACHUTE BASED ON CONSTRUCTION AREA, $S_c$ (NOMINAL POROSITY = 10 $ft^3/ft^2$-min)

| $\alpha$ | 0 | ±2 | ±4 | ±6 | ±8 | ±10 |
|---|---|---|---|---|---|---|
| $C_M$ | .0 | ∓0.046 | ∓0.092 | -0.147 | -0.197 | -0.214 |
| $C_N$ | .0 | ∓0.037 | ∓0.075 | -0.119 | -0.161 | -0.174 |
| $C_T$ | 0.733 | 0.724 | 0.725 | 0.691 | 0.729 | 0.712 |

M=0.5

| $\alpha$ | 0 | ±2 | ±4 | ±6 | ±8 | ±10 |
|---|---|---|---|---|---|---|
| $C_M$ | .0 | ∓0.047 | ∓0.095 | -0.144 | -0.191 | -0.238 |
| $C_N$ | .0 | ∓0.038 | ∓0.077 | -0.117 | -0.155 | -0.194 |
| $C_T$ | 0.915 | 0.896 | 0.880 | 0.846 | 0.837 | 0.822 |

M=0.8

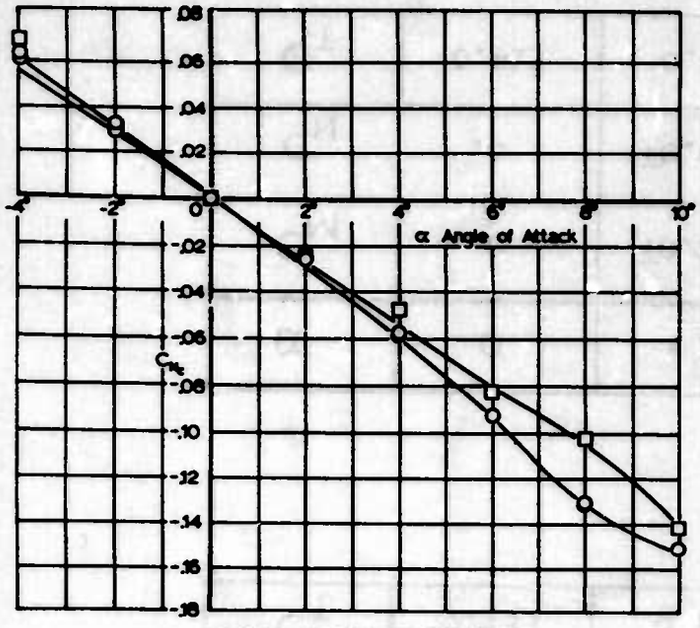


NORMAL FORCE COEFFICIENT

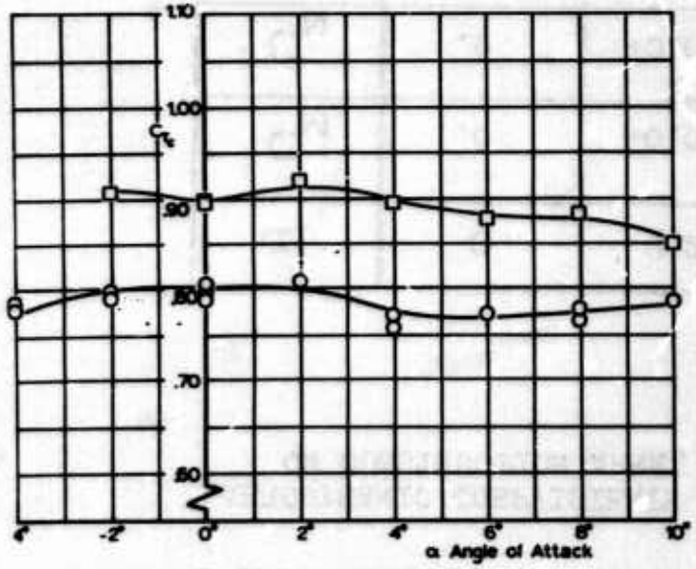


TANGENT FORCE COEFFICIENT

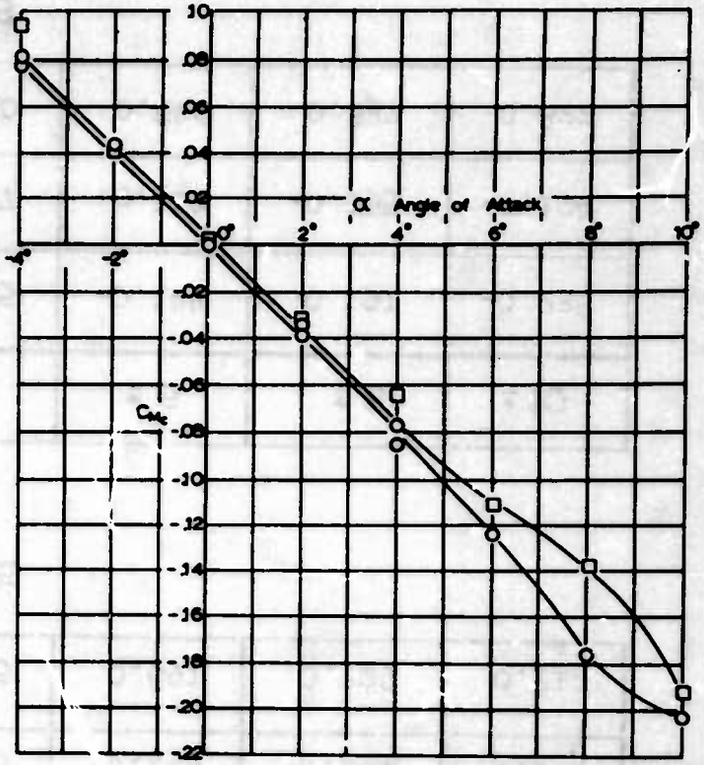


MOMENT COEFFICIENT

○ M=0.5 Re = $1.3 \times 10^6$
□ M=0.8 Re = $1.9 \times 10^6$

Fig 24. Aerodynamic Coefficients vs. Angle of Attack for Ribbed Guide Surface Parachute ( Nominal Porosity = 30 $ft^3/ft^2$ min )

TABLE 8

AERODYNAMIC COEFFICIENTS FOR RIBBED GUIDE SURFACE PARACHUTE BASED ON CONSTRUCTION AREA, $S_c$ (NOMINAL POROSITY = 30 $ft^3/ft^2$-min)

| $\alpha$ | 0 | ±2 | ±4 | +6 | +8 | +10 |
|---|---|---|---|---|---|---|
| $C_M$ | .0 | ∓0.039 | ∓0.081 | -0.124 | -0.175 | -0.223 |
| $C_N$ | .0 | ∓0.029 | ∓0.060 | -0.092 | -0.130 | -0.151 |
| $C_T$ | 0.795 | 0.799 | 0.774 | 0.772 | 0.773 | 0.787 |

M=0.5

| $\alpha$ | 0 | ±2 | ±4 | +6 | +8 | +10 |
|---|---|---|---|---|---|---|
| $C_M$ | .0 | ∓0.037 | ∓0.086 | -0.112 | -0.138 | -0.192 |
| $C_N$ | .0 | ∓0.027 | ∓0.063 | -0.082 | -0.101 | -0.141 |
| $C_T$ | 0.896 | 0.914 | 0.894 | 0.878 | 0.883 | 0.850 |

M=0.8

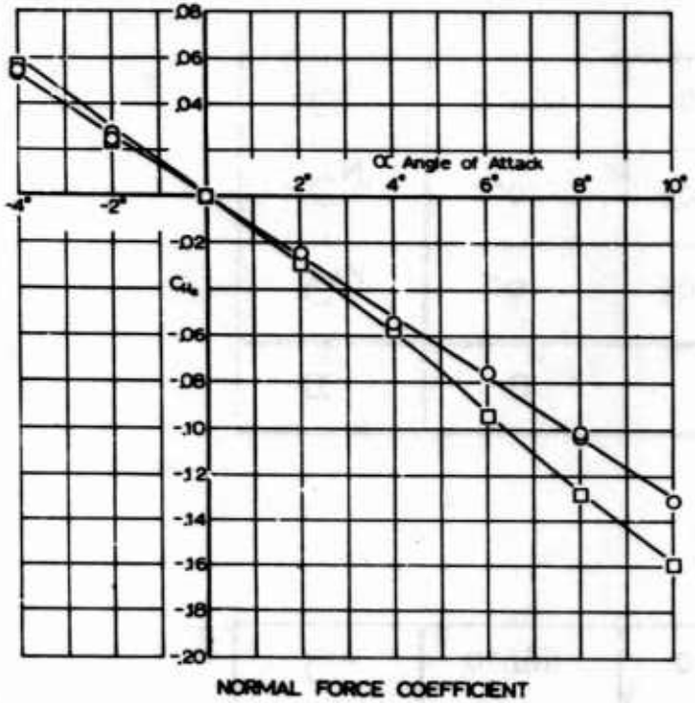


NORMAL FORCE COEFFICIENT

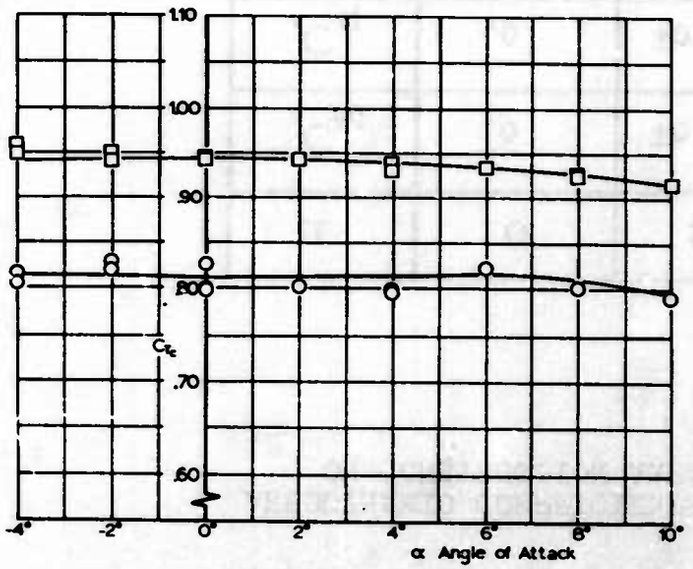


TANGENT FORCE COEFFICIENT

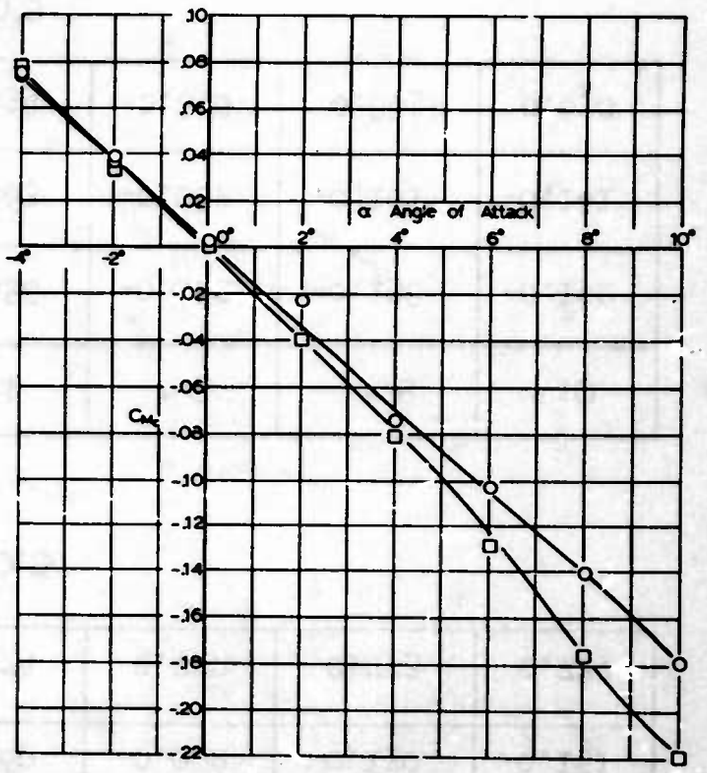


MOMENT COEFFICIENT

○ M=0.5 Re = 1.3 x $10^6$
□ M=0.8 Re = 1.9 x $10^6$

Fig 25. Aerodynamic Coefficients vs. Angle of Attack for Ribbed Guide Surface Parachute (Nominal Porosity = 60 $ft^3/ft^2$ min)

TABLE 9

AERODYNAMIC COEFFICIENTS FOR RIBBED GUIDE SURFACE PARACHUTE BASED ON CONSTRUCTION AREA, $S_c$ (NOMINAL POROSITY = 60 $ft^3/ft^2$-min)

| $\alpha$ | 0 | ±2 | ±4 | +6 | +8 | +10 |
|---|---|---|---|---|---|---|
| $C_M$ | .0 | ∓0.035 | ∓0.074 | -0.104 | -0.139 | -0.179 |
| $C_N$ | .0 | ∓0.026 | ∓0.054 | -0.076 | -0.102 | -0.131 |
| $C_T$ | 0.806 | 0.818 | 0.804 | 0.824 | 0.803 | 0.792 |

M = 0.5

| $\alpha$ | 0 | ±2 | ±4 | +6 | +8 | +10 |
|---|---|---|---|---|---|---|
| $C_M$ | .0 | ∓0.036 | ∓0.078 | -0.129 | -0.177 | -0.219 |
| $C_N$ | .0 | ∓0.026 | ∓0.057 | -0.094 | -0.129 | -0.160 |
| $C_T$ | 0.944 | 0.946 | 0.945 | 0.935 | 0.927 | 0.916 |

M = 0.8

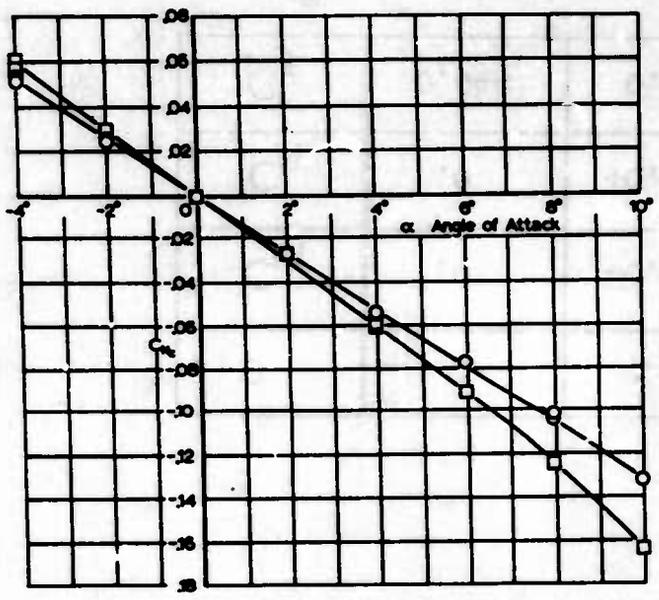


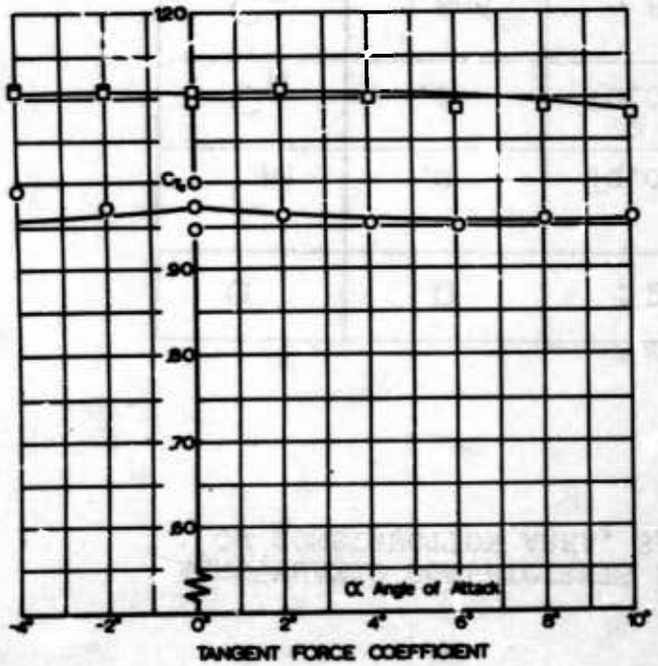


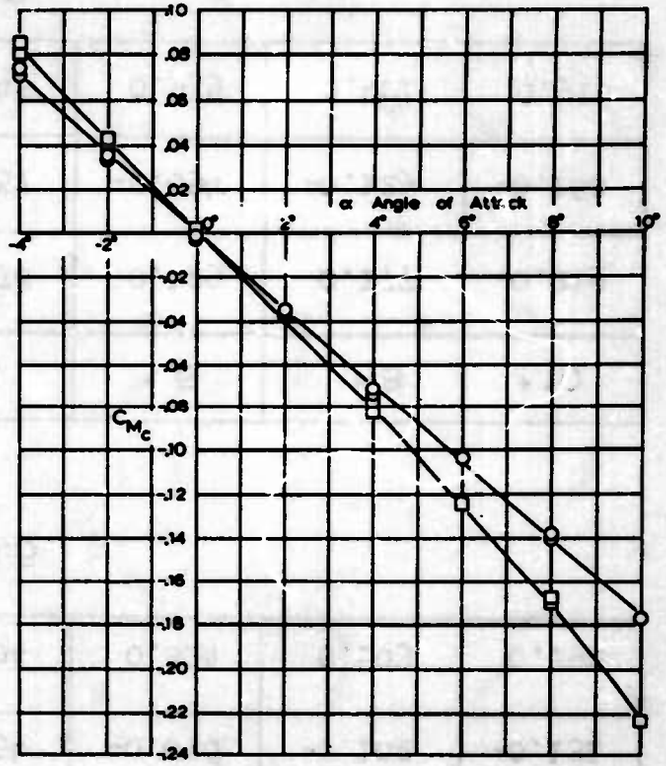


Fig 26. Aerodynamic Coefficients vs. Angle of Attack for Ribbed Guide Surface Parachute ( Nominal Porosity = 120 ft³ / ft² min)

TABLE 10

AERODYNAMIC COEFFICIENTS FOR RIBBED GUIDE SURFACE PARACHUTE BASED ON CONSTRUCTION AREA, $S_c$ (NOMINAL POROSITY = 120 $ft^3/ft^2$-min)

| $\alpha$ | 0 | ±2 | ±4 | +6 | +8 | +10 |
|---|---|---|---|---|---|---|
| $C_M$ | .0 | ∓0.035 | ∓0.072 | -0.104 | -0.140 | -0.179 |
| $C_N$ | .0 | ∓0.026 | ∓0.053 | -0.076 | -0.103 | -0.131 |
| $C_T$ | 0.972 | 0.961 | 0.968 | 0.950 | 0.966 | 0.960 |

M = 0.5

| $\alpha$ | 0 | ±2 | ±4 | +6 | +8 | +10 |
|---|---|---|---|---|---|---|
| $C_M$ | .0 | ∓0.039 | ∓0.081 | -0.124 | -0.169 | -0.224 |
| $C_N$ | .0 | ∓0.028 | ∓0.059 | -0.090 | -0.123 | -0.163 |
| $C_T$ | 1.109 | 1.111 | 1.111 | 1.088 | 1.093 | 1.082 |

M = 0.8

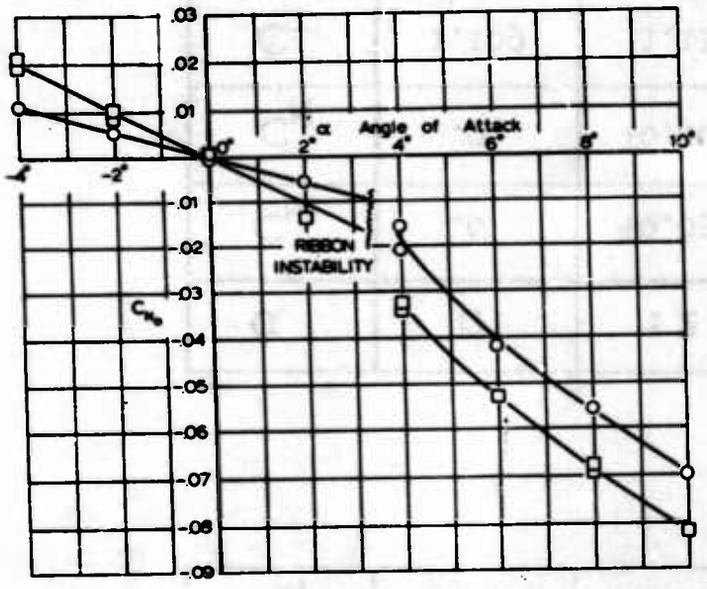


NORMAL FORCE COEFFICIENT -

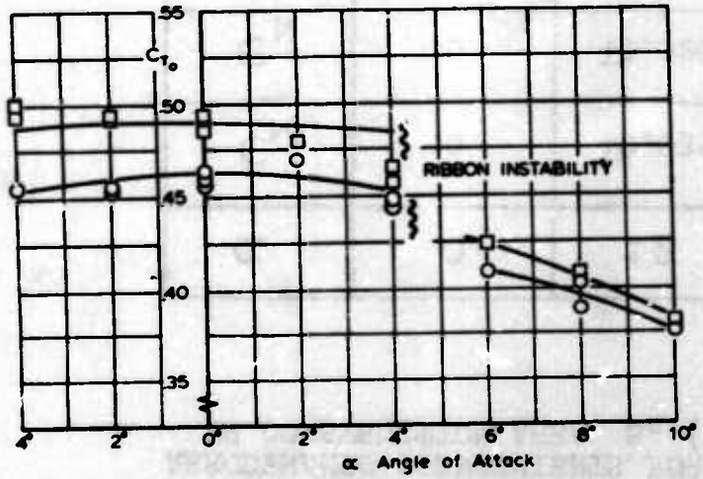


TANGENT FORCE COEFFICIENT

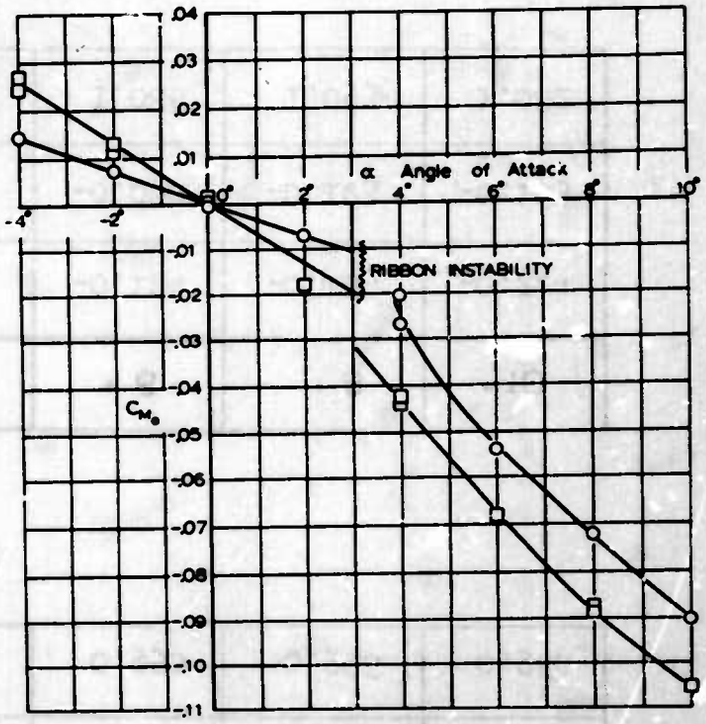


MOMENT COEFFICIENT

○ M=0.5 Re = 1.3 x $10^6$
□ M=0.8 Re = 1.9 x $10^6$

Fig 27. Aerodynamic Coefficients vs. Angle of Attack for Ribbon Parachute ( 50 in. Prototype )

TABLE 11

AERODYNAMIC COEFFICIENTS FOR 50 IN. PROTOTYPE RIBBON PARACHUTE BASED ON NOMINAL AREA, $S_o$

| $\alpha$ | 0 | ±2 | ±4 | ±6 | ±8 | ±10 |
|---|---|---|---|---|---|---|
| $C_M$ | .0 | ∓0.007 | ∓0.019 | -0.052 | -0.072 | -0.090 |
| $C_N$ | .0 | ∓0.006 | ∓0.015 | -0.041 | -0.056 | -0.070 |
| $C_T$ | 0.460 | 0.459 | 0.449 | 0.410 | 0.395 | 0.376 |

M=0.5

| $\alpha$ | 0 | ±2 | ±4 | ±6 | ±8 | ±10 |
|---|---|---|---|---|---|---|
| $C_M$ | .0 | ∓0.013 | ∓0.036 | -0.068 | -0.089 | -0.106 |
| $C_N$ | .0 | ∓0.010 | ∓0.027 | -0.053 | -0.069 | -0.082 |
| $C_T$ | 0.490 | 0.489 | 0.479 | 0.424 | 0.408 | 0.379 |

M=0.8

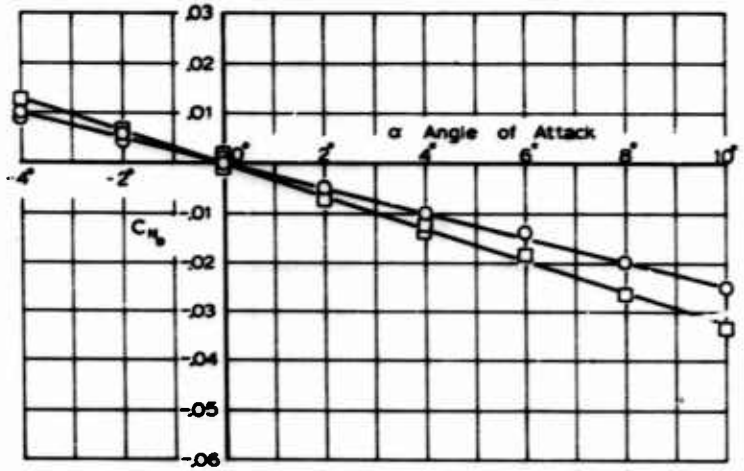


NORMAL FORCE COEFFICIENT

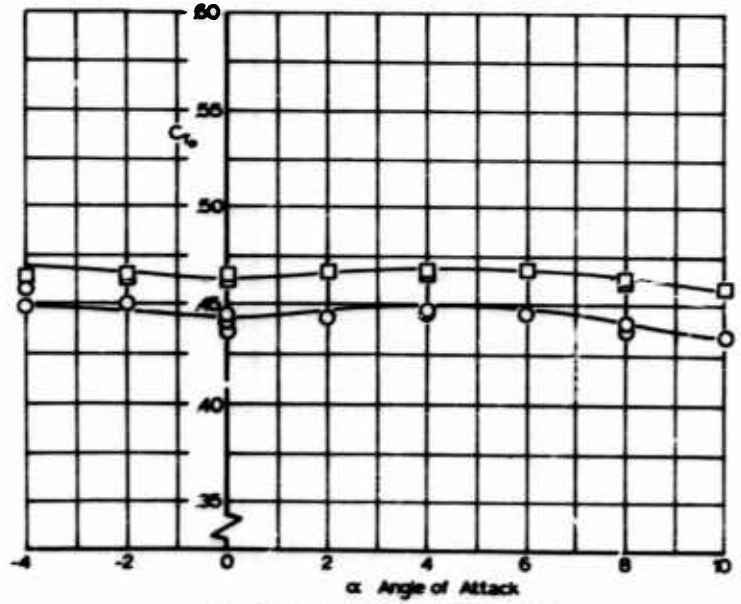


TANGENT FORCE COEFFICIENT

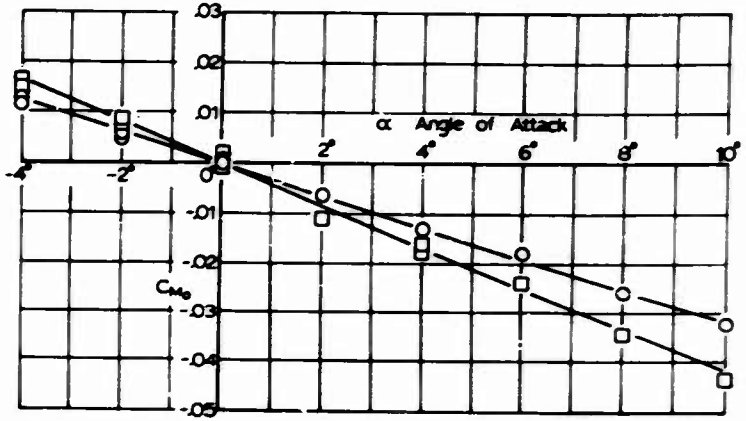


MOMENT COEFFICIENT

○ M=0.5 Re = 1.3 x $10^6$
□ M=0.8 Re = 1.9 x $10^6$

Fig 28. Aerodynamic Coefficients vs. Angle of Attack for Ribbon Parachute (100 in. Prototype)

TABLE 12

AERODYNAMIC COEFFICIENTS FOR 100 IN PROTOTYPE RIBBON PARACHUTE BASED ON NOMINAL AREA, $S_o$

| $\alpha$ | 0 | ±2 | ±4 | ±6 | ±8 | ±10 |
|---|---|---|---|---|---|---|
| $C_M$ | .0 | ∓0.006 | ∓0.013 | -0.019 | -0.026 | -0.032 |
| $C_N$ | .0 | ∓0.005 | ∓0.010 | -0.015 | -0.020 | -0.025 |
| $C_T$ | 0.441 | 0.446 | 0.449 | 0.446 | 0.439 | 0.435 |

M = 0.5

| $\alpha$ | 0 | ±2 | ±4 | ±6 | ±8 | ±10 |
|---|---|---|---|---|---|---|
| $C_M$ | .0 | ∓0.008 | ∓0.017 | -0.026 | -0.034 | -0.042 |
| $C_N$ | .0 | ∓0.006 | ∓0.013 | -0.020 | -0.026 | -0.033 |
| $C_T$ | 0.463 | 0.465 | 0.463 | 0.468 | 0.463 | 0.459 |

M = 0.8

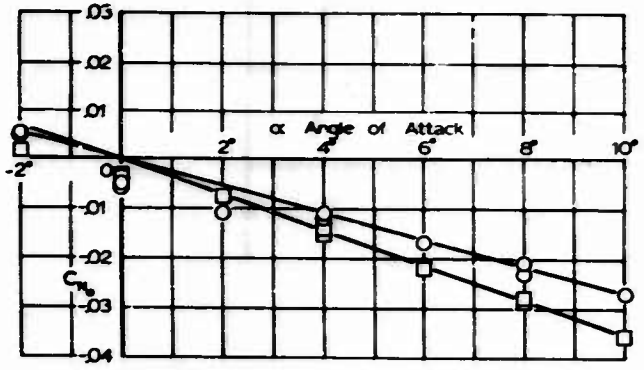


NORMAL FORCE COEFFICIENT

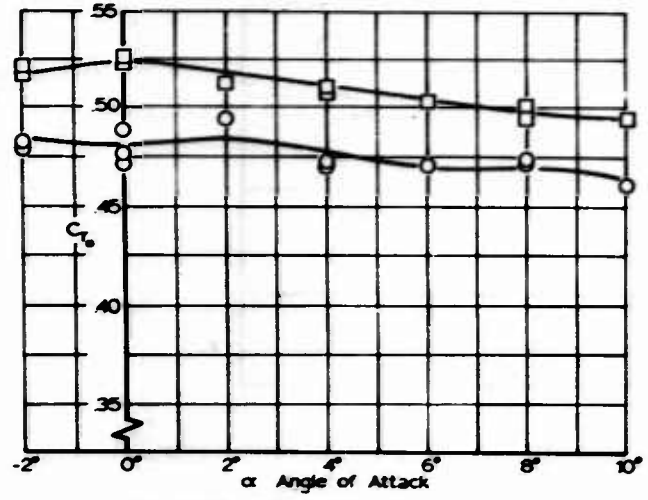


TANGENT FORCE COEFFICIENT

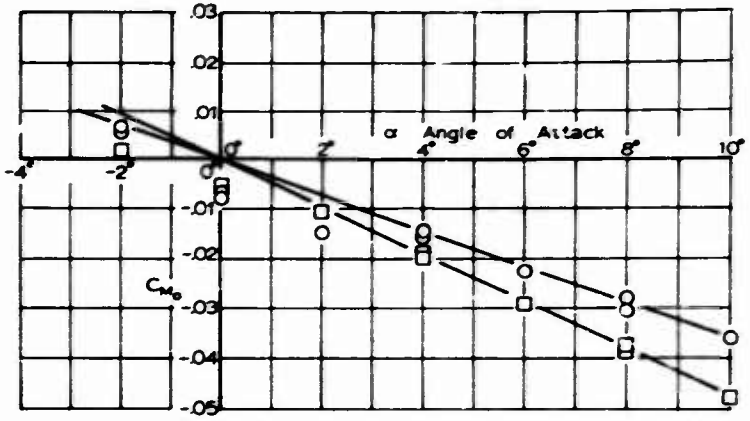


MOMENT COEFFICIENT

○ M=0.5 Re = $1.3 \times 10^6$
□ M=0.8 Re = $1.9 \times 10^6$

Fig 29. Aerodynamic Coefficients vs. Angle of Attack for Ringslot Parachute (50 in. Prototype)

TABLE 13

AERODYNAMIC COEFFICIENTS FOR 50 IN. PROTOTYPE RINGSLOT PARACHUTE BASED ON NOMINAL AREA, $S_o$

| $\alpha$ | 0 | ± 2 | ± 4 | ± 6 | ± 8 | ± 10 |
|---|---|---|---|---|---|---|
| $C_M$ | .0 | ∓0.007 | ∓0.015 | -0.021 | -0.028 | -0.036 |
| $C_N$ | .0 | ∓0.006 | ∓0.011 | -0.016 | -0.021 | -0.027 |
| $C_T$ | 0.479 | 0.484 | 0.471 | 0.468 | 0.471 | 0.462 |

M = 0.5

| $\alpha$ | 0 | ± 2 | ± 4 | ± 6 | ± 8 | ± 10 |
|---|---|---|---|---|---|---|
| $C_M$ | .0 | ∓0.009 | ∓0.019 | -0.028 | -0.037 | -0.047 |
| $C_N$ | .0 | ∓0.007 | ∓0.014 | -0.021 | -0.028 | -0.036 |
| $C_T$ | 0.526 | 0.517 | 0.509 | 0.502 | 0.497 | 0.494 |

M = 0.8

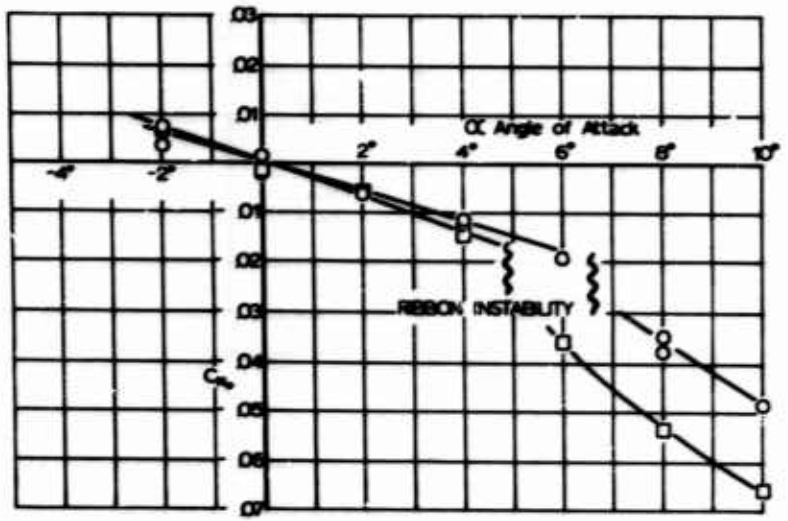


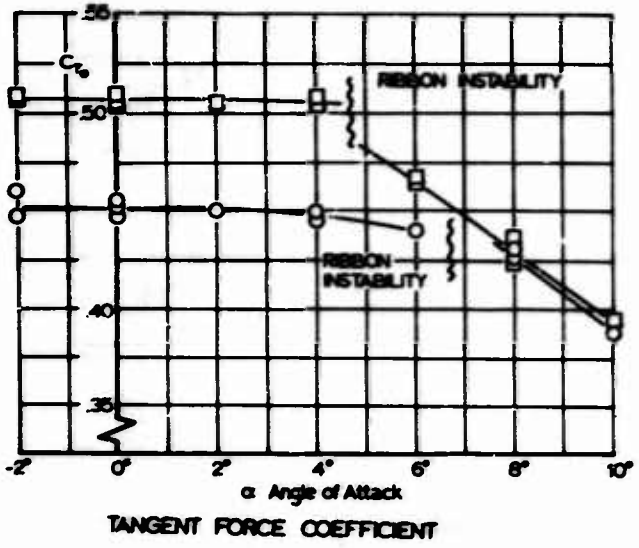


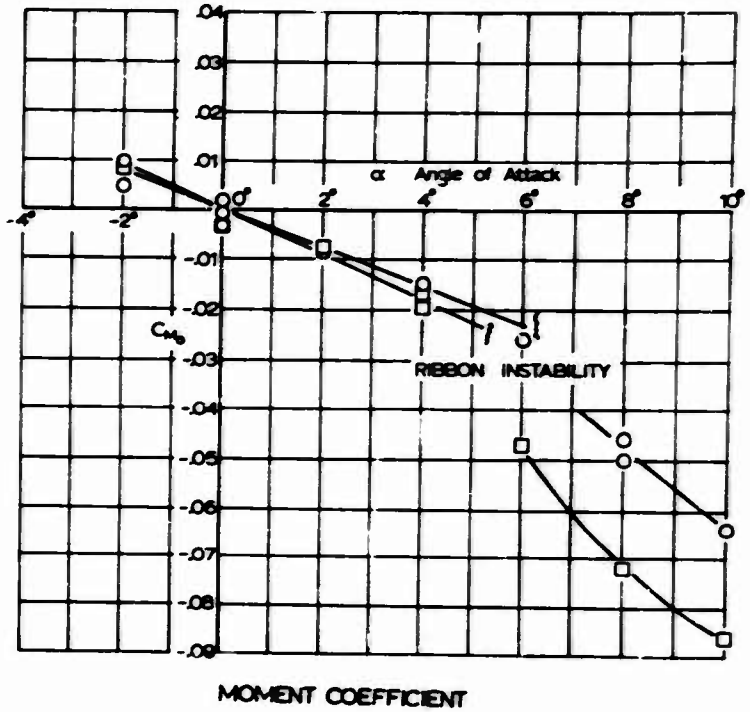


○ M=0.5 Re = $1.3 \times 10^6$
□ M=0.8 Re = $1.9 \times 10^6$

Fig 30. Aerodynamic Coefficients vs. Angle of Attack for Ringslot Parachute (100 in. Prototype)

TABLE 14

AERODYNAMIC COEFFICIENTS FOR 100 IN. PROTOTYPE RINGSLOT PARACHUTE, BASED ON NOMINAL AREA, $S_o$

| $\alpha$ | 0 | ± 2 | ± 4 | ± 6 | ± 8 | ±10 |
|---|---|---|---|---|---|---|
| $C_M$ | .0 | ∓0.008 | ∓0.019 | -0.023 | -0.048 | -0.064 |
| $C_N$ | .0 | ∓0.006 | ∓0.015 | -0.018 | -0.036 | -0.049 |
| $C_T$ | 0.449 | 0.453 | 0.447 | 0.440 | 0.427 | 0.387 |

M=0.5

| $\alpha$ | 0 | ± 2 | ± 4 | ± 6 | ± 8 | ±10 |
|---|---|---|---|---|---|---|
| $C_M$ | .0 | ∓0.010 | ∓0.018 | -0.047 | -0.070 | -0.086 |
| $C_N$ | .0 | ∓0.007 | ∓0.014 | -0.036 | -0.054 | -0.066 |
| $C_T$ | 0.502 | 0.503 | 0.500 | 0.456 | 0.417 | 0.393 |

M=0.8

Unclassified

Security Classification

**DOCUMENT CONTROL DATA - R&D**

*(Security classification of title, body of abstract and indexing annotation must be entered when the overall report is classified)*

1. ORIGINATING ACTIVITY (Corporate author)
University of Minnesota
Minneapolis 14, Minnesota

2a. REPORT SECURITY CLASSIFICATION
Unclassified

2b. GROUP
n/a

3. REPORT TITLE
Drag and Stability of Guide Surface, Ribbon, and Ringslot Parachutes at High Subsonic Speeds

4. DESCRIPTIVE NOTES (Type of report and inclusive dates)
Final Report April 63 - March 65

5. AUTHOR(S) (Last name, first name, initial)
Haak, E. L.
Hubert, R. J.

6. REPORT DATE
September 1965

7a. TOTAL NO. OF PAGES
53

7b. NO. OF REFS
3

8a. CONTRACT OR GRANT NO. AF33(657)-11184

b. PROJECT NO. 6065

c. Task No 606503

d.

9a. ORIGINATOR'S REPORT NUMBER(S)
AFFDL-TR-65-108

9b. OTHER REPORT NO(S) (Any other numbers that may be assigned this report)
none

10 AVAILABILITY/LIMITATION NOTICES
Qualified users may obtain copies of this report from DDC. DDC release to CFSTI is not authorized. Foreign announcement and dissemination of this report is not authorized.

11. SUPPLEMENTARY NOTES
none

12. SPONSORING MILITARY ACTIVITY
AFFDL (FDFR)
WPAFB, Ohio

13. ABSTRACT

Four conventional type parachutes; namely, a ribbed and a ribless guide surface parachute and a ribbon and ringslot parachute were tested at Mach numbers of 0.5 and 0.8 to establish their drag and stability characteristics and to evaluate their general performance in this Mach number range. In all cases the parachute models were stable and their drag coefficient increased slightly with increasing Mach number.

It was found that both the drag and the stability of the guide surface type parachutes change with cloth porosity.

Tests also indicate that for both the ribbed and ribless guide surface parachutes, the tangent force coefficient increases with increasing stagnation pressure at a constant Mach number, and while the stability of the ribless guide surface parachute increases, that of the ribbed type is essentially unchanged.

Tests on ribbon and ringslot parachutes of equal geometric porosity indicate that while the drag increases as the ribbon width increases, the stability of these parachutes does not change significantly with wider ribbons.

The moment coefficients of guide surface parachutes and their derivations with respect to the angle of attack were in all cases higher than the comparative values of the ribbon or ringslot parachutes.

DD FORM 1 JAN 64 1473

Unclassified

Security Classification

Unclassified

Security Classification

| 14. KEY WORDS | LINK A | | LINK B | | LINK C | |
|---|---|---|---|---|---|---|
| | ROLE | WT | ROLE | WT | ROLE | WT |
| Drag<br>Stability<br>Ribbon Canopies<br>Ringslot Canopies<br>Guide Surface Canopies<br>Wind Tunnel Tests<br>Mach Nrs of 0.5 and 0.8 | | | | | | |

## INSTRUCTIONS

1. **ORIGINATING ACTIVITY:** Enter the name and address of the contractor, subcontractor, grantee, Department of Defense activity or other organization *(corporate author)* issuing the report.

2a. **REPORT SECURITY CLASSIFICATION:** Enter the overall security classification of the report. Indicate whether "Restricted Data" is included. Marking is to be in accordance with appropriate security regulations.

2b. **GROUP:** Automatic downgrading is specified in DoD Directive 5200.10 and Armed Forces Industrial Manual. Enter the group number. Also, when applicable, show that optional markings have been used for Group 3 and Group 4 as authorized.

3. **REPORT TITLE:** Enter the complete report title in all capital letters. Titles in all cases should be unclassified. If a meaningful title cannot be selected without classification, show title classification in all capitals in parenthesis immediately following the title.

4. **DESCRIPTIVE NOTES:** If appropriate, enter the type of report, e.g., interim, progress, summary, annual, or final. Give the inclusive dates when a specific reporting period is covered.

5. **AUTHOR(S):** Enter the name(s) of author(s) as shown on or in the report. Enter last name, first name, middle initial. If military, show rank and branch of service. The name of the principal author is an absolute minimum requirement.

6. **REPORT DATE:** Enter the date of the report as day, month, year; or month, year. If more than one date appears on the report, use date of publication.

7a. **TOTAL NUMBER OF PAGES:** The total page count should follow normal pagination procedures, i.e., enter the number of pages containing information.

7b. **NUMBER OF REFERENCES:** Enter the total number of references cited in the report.

8a. **CONTRACT OR GRANT NUMBER:** If appropriate, enter the applicable number of the contract or grant under which the report was written.

8b, 8c, & 8d. **PROJECT NUMBER:** Enter the appropriate military department identification, such as project number, subproject number, system numbers, task number, etc.

9a. **ORIGINATOR'S REPORT NUMBER(S):** Enter the official report number by which the document will be identified and controlled by the originating activity. This number must be unique to this report.

9b. **OTHER REPORT NUMBER(S):** If the report has been assigned any other report numbers *(either by the originator or by the sponsor)*, also enter this number(s).

10. **AVAILABILITY/LIMITATION NOTICES:** Enter any limitations on further dissemination of the report, other than those imposed by security classification, using standard statements such as:

(1) "Qualified requesters may obtain copies of this report from DDC."

(2) "Foreign announcement and dissemination of this report by DDC is not authorized."

(3) "U. S. Government agencies may obtain copies of this report directly from DDC. Other qualified DDC users shall request through _____."

(4) "U. S. military agencies may obtain copies of this report directly from DDC. Other qualified users shall request through _____."

(5) "All distribution of this report is controlled. Qualified DDC users shall request through _____."

If the report has been furnished to the Office of Technical Services, Department of Commerce, for sale to the public, indicate this fact and enter the price, if known.

11. **SUPPLEMENTARY NOTES:** Use for additional explanatory notes.

12. **SPONSORING MILITARY ACTIVITY:** Enter the name of the departmental project office or laboratory sponsoring *(paying for)* the research and development. Include address.

13. **ABSTRACT:** Enter an abstract giving a brief and factual summary of the document indicative of the report, even though it may also appear elsewhere in the body of the technical report. If additional space is required, a continuation sheet shall be attached.

It is highly desirable that the abstract of classified reports be unclassified. Each paragraph of the abstract shall end with an indication of the military security classification of the information in the paragraph, represented as *(TS), (S), (C), or (U)*.

There is no limitation on the length of the abstract. However, the suggested length is from 150 to 225 words.

14. **KEY WORDS:** Key words are technically meaningful terms or short phrases that characterize a report and may be used as index entries for cataloging the report. Key words must be selected so that no security classification is required. Identifiers, such as equipment model designation, trade name, military project code name, geographic location, may be used as key words but will be followed by an indication of technical context. The assignment of links, rules, and weights is optional.

Unclassified

Security Classification